

**Neointima formation on a synthetic vascular graft with altered luminal  
surface geometry following g-force endothelial cell seeding**

A THESIS  
SUBMITTED TO THE FACULTY OF THE GRADUATE SCHOOL  
OF THE UNIVERSITY OF MINNESOTA  
BY

Michael F. Wolf

IN PARTIAL FULFILLMENT OF THE REQUIREMENTS  
FOR THE DEGREE OF  
MASTER OF SCIENCE

Richard Bianco and Paul A Iaizzo, Advisors

December, 2009

© Michael F. Wolf 2009

## Acknowledgements

I would like to first acknowledge the tremendous professional and technical assistance of Laurie Yunker. Ms. Yunker played a critical role in the majority of laboratory in vitro cell work and follow-up in vivo studies that make up the investigations in this report. I must also acknowledge the many years of support and guidance from Dr. Jim Anderson at Case Western Reserve University. Dr. Anderson has been an invaluable advisor and mentor for almost 20 years on a wide range of topics dealing with evaluation of biological responses of medical devices and materials. Dr. Anderson provided the analysis and critical review of the histological finding in the in vivo portion of this investigation. I must also acknowledge and mention my tremendous appreciation for the input and guidance of Johann Meinhart, who provided technical consultation and helped rate the SEM evaluations in the investigation. Dr. Meinhart has been an absolutely critical player in the field of clinical endothelialization of vascular prostheses and his feedback and professional guidance in these studies has been invaluable and immensely appreciated. Acknowledgment would not be complete without mentioning the tremendous guidance and career-long professional support of Paul Trescony. Paul's ideas are spread throughout this work and he lent a critical hand in the review of the SEM work in the investigation. Paul also assisted in the advice and guidance of Nicolas Rivron who did a fabulous job in the early development and characterization of the brushing process to make bePTFE. I must also acknowledge the tremendous professional support of the staff at the Medtronic Physiological Research Laboratory whose contributions and dedication lead to the in vivo portion of the investigation being conducted in the most professional and the most humane manner. I would also like to acknowledge and thank Medtronic Inc. for its support and funding of the investigations. This work certainly also needs to acknowledge the kind support from KipsBay Medical and Mr. Manny Villafana, the owners and ongoing developers of the material and cell seeding technology reviewed in this thesis.

Last but not least I would like to acknowledge Richard Bianco, Paul Iaizzo, and Bob Tranquillo for their kind support and professional guidance on this thesis.

## **Dedication**

I first wish to dedicate this thesis to my parents, Don and Katy Wolf. Their lifelong love and support, and their attitude toward life, kindness, and commitment (and so much more) helped make this possible. I love you, and I miss you. I would also like to dedicate this work to my children Maggie, Liesl, and Natalie, and to my most special ‘fence’ Michèle Coppin. Each of these special individuals knows how I have come to say that in life one continually alternates between being a student, and being a teacher. Their kind support, words of encouragement, and patience in this latest effort as a student made it seem all the more possible. In reality, they helped me to make it happen.

Finally, I also wish to dedicate this work to my special friend, Andreas Zisch, who has been like a brother to me. Each time I climb in the mountains, and indeed whenever I face something that challenges me, I will be thinking of you my friend.

## Abstract

Finding an effective small diameter synthetic vascular graft has been the focus of research for over three decades. A major direction has been on a means to establish a functional endothelial cell (EC) lining on common graft materials. Unfortunately, a simple operating room (OR) method has proven to be neither obvious to knowledgeable researchers nor feasible for standard hospital staff. In the space of the host of variables considered by researchers, the goal of this work was to see if a more practicable procedure might be identified using a series of factorial experimental design evaluations on certain process-simplifying and material-alteration concepts. These concepts were micro-geometric surface modification, g-force cell seeding, and graft pretreatment using a particular fraction of autologous blood. For this, clinical ePTFE graft material was surface-modified into 'brushed' ePTFE (bePTFE) to make the material more receptive to cell uptake and adhesion; seeding graft materials with ECs was achieved using high g-force from axial centrifugation; and, a graft pretreatment with autologous platelet poor plasma was used to generate an autologous fibrin-platelet-poor layer (aFPPL) on the graft surface. The goal of this approach was to rapidly identify, assess, and optimize the most minimal-impact conditions applicable in an operating room that positively influence formation of a healthy autologous cell lining. Bench top studies revealed the bePTFE material to show an increased uptake and retention of ECs compared to ePTFE ( $P < 0.05$ ). In addition, independent of material, the use of high rpm g-force seeding compared to seeding under slow rotation resulted in significantly more cells taken up by the materials

under high g-force ( $P < 0.05$ ). The cells also appeared to be retained under simulated pulsatile flow conditions. Five day tissue culture experiments then showed that an aFPPL layer applied to the graft surface prior to g-force cell seeding was a substantial growth matrix for seeded cells. A follow-up in vivo  $2^4$  factorial experimental design study on graft material, EC seeding via g-force, pretreatment generating an aFPPL, and graft orientation indicated the following trends and significant observations: (1) bePTFE was associated with a trend in improved patency ( $P < 0.07$ ), reduced histological evidence of thrombosis ( $P < 0.08$ ), and reduced luminal red discolorations ( $P < 0.0001$ ), (2) EC seeding was shown to be associated with a trend in improved patency ( $P < 0.08$ ), a reduction in surface discoloration ( $P < 0.0004$ ), and an increased midgraft endothelium ( $P < 0.04$ ) assessed by scanning electron microscopy (SEM). Histology scores also revealed EC seeding to be associated with more neointimal development ( $P < 0.08$ ), more graft cellularity ( $P < 0.001$ ), and higher macrophage infiltration ( $P < 0.007$ ); and (3) graft pretreatment with autologous PPP to generate an aFPPL on the graft surface showed a significant impact on the surface discoloration ( $P < 0.009$ ) and extent of endothelial cell coverage ( $P < 0.01$ ) as assessed by SEM. This work demonstrates that through a multi-parameter screening study approach a number of potential significant improvements towards a practicable one-step OR-compatible vascular graft endothelialization technique were identified.

## Table of Contents

<b>List of Tables</b>	Page vi
<b>List of Figures</b>	vii-viii
<b>INTRODUCTION</b>	1
<b>MATERIALS and METHODS</b>	8
Expanded polytetrafluoroethylene (ePTFE) and brushed graft materials	8
Chemical and Physical Characterization	9
Cell preparations and seeding considerations	10
Design and principle of an axial centrifuge cell seeding system	12
Cell uptake and cell viability assessment	14
In vitro studies to identify influential factors in endothelial cell uptake/seeding on graft materials	14
In vitro cell culture studies to identify graft pre-seeding treatments that support endothelial cell growth	17
Vein harvest, autologous endothelial cell stripping, and simulated OR cell seeding	18
In vivo graft implantation study	19
In vivo study design	19
Gross and histopathology assessments	21
Scanning electron microscopy (SEM) assessment of endothelial seeding and coverage	22
Statistical Analyses	23
<b>RESULTS</b>	24
Graft Material Characterization	24
Surface Topography	24
Surface Chemistry and Physical Properties	24
Axial Centrifugation Cell Seeding	26
In vitro studies for factors influential to endothelial cell uptake/seeding and growth	27
In vivo vein harvesting, endothelial cell stripping, and mock OR seeding	30
In vivo graft implantation study	
Gross and histological observations	36
Scanning electron microscopy observations	40
<b>DISCUSSION and CONCLUSIONS</b>	43
<b>BIBLIOGRAPHY</b>	61

## List of Tables

		Page
Table 1	Graft material chemical and physical properties	26
Table 2	Factorial experimental design studies for endothelial cell (EC) growth on synthetic graft materials	30
Table 3	Summary of graft patency observed in the in vivo implant study	37



## List of Figures

	Page	
Figure 1	The Mansfield-Herring single-stage operating room vascular graft seeding procedure to apply venous endothelial cells to a vascular graft surface.	5
Figure 2	Schematic of the ‘two-stage’ approach to seeding a vascular graft with autologous endothelial cells	6
Figure 3	Scanning electron micrograph of standard ePTFE and brushed ePTFE (bePTFE).	7
Figure 4	Scanning electron micrograph of arterial endothelium	11
Figure 5	Axial rotation of the tubular vascular graft under high speed rotation	13
Figure 6	In vitro pulsatile flow tissue culture model	16
Figure 7	Representative factorial experimental designs for characterizing and optimizing uptake of ECs on graft surfaces	17
Figure 8	Geometric representation of the main in vivo study factorial experimental design	21
Figure 9	Effect of variables on uptake of endothelial cells on graft materials over a range of experimental conditions	28-29
Figure 10	Cell harvesting efficiency and geometric representation of the in vivo cell harvesting factorial experimental design	32
Figure 11	Representative scanning electron micrographs showing the variation in enzymatic cell removal	33
Figure 12	Representative Live/Dead assay images of graft materials receiving PPP treatment and g-force seeding of canine venous endothelial cells.	34

Figure 13	Scanning electron micrographs of ePTFE and bePTFE following axial centrifugation cell seeding and exposure to platelet poor plasma (PPP) to form an autologous fibrin platelet poor layer (aFPPL).	35
Figure 14	Representative gross photographic images of patent grafts in each main test category	38
Figure 15	Representative H&E histology sections taken at the midgraft region of patent ePTFE and bePTFE grafts	39
Figure 16	A representative low magnification SEM montage showing a complete graft hemisection, and higher magnification images and the graft segmenting scheme	41
Figure 17	Representative SEM micrographs taken at the midgraft region of patent ePTFE and bePTFE vascular grafts	42
Figure 18	Graphical summary of SEM scores by treatment group and along the entire length of patent grafts	43
Figure 19	Representative SEM micrographs showing an on-edge cut revealing the variation in morphology and thickness of the autologous fibrin-platelet-poor layer (aFPPL).	51
Figure 20	Representative SEM montages of control bePTFE and ePTFE explant, and, average SEM scores along control grafts and grafts receiving PPP treatment and cell seeding.	53
Figure 21	Schematic representation of a possible practicable new single-stage approach to seeding synthetic grafts in the operating room with autologous cells.	60

## INTRODUCTION

It has been over thirty years since Mansfield, Herring, and their co-workers first suggested that an *in vitro* lining of a synthetic vascular graft with a host's own endothelial cells may retard thrombus formation and lead to improved graft patency [1, 2]. Since then a series of small human clinical studies extending into this decade [3-5] has taken place and this hypothesis has been demonstrated in both peripheral [6] and coronary [7] applications. Thus, a combination of a standard material plus living autologous cells, perhaps the first true demonstrated application of tissue engineering, has been shown to significantly improve the performance of a synthetic vascular graft. As with other, albeit rare, demonstrated applications in tissue engineering [8], the process of showing benefit and establishing approval and adoption of such technology has proven to be a protracted and demanding undertaking.

Notably, the ultimate clinical protocol used to establish an autologous endothelial cell lining on a graft deviates significantly from the original Mansfield-Herring vision of a single stage procedure taking place in the operating room (OR) (Figure 1). Because of poor to mixed results in 'single stage' OR procedures, the ultimate clinical protocol evolved into a two-stage procedure that couples routine activities that take place in the operating room with routine activities that take place in a tissue culture laboratory (Figure 2). The procedure starts in the operating room with the harvesting of a nonessential host vein for its endothelial cells. Cell removal (stripping), expansion of cells in culture, and

seeding of these cells onto the graft then take place in a nearby tissue culture laboratory [9]. Seeding cells onto a matrix of proteins followed by an incubation period are additional steps in the process recognized to assist with initial attachment and subsequent growth and maturation of cells on the graft material [6, 10]. The procedure is completed, approximately thirty days from vein harvest, upon return to the OR with implantation of the endothelial-lined graft into the patient. The later is performed using standard surgical technique, with added care taken to ensure the graft remains moist to protect the cells. These procedures undeniably form a neointima on the synthetic graft [11-13], with performance appearing to be at least equivalent to autologous vein and distinctly improved over the non-cell-lined graft. Still, the deviations from Mansfield and Herring's original suggestion of a single OR procedure have come with consequences: (1) the patient is presented with two invasive procedures rather than one (2) the process is not amenable to cases requiring immediate care (3) patient tissue leaves the operating room for an extended period, receives certain manipulations, and requires expertise in handling and tissue culture not normally present in the hospital setting, and (4) the regulatory hurdles for adoption of the procedure are complex. These drawbacks, in face of the distinctly favorable outcome, have contributed to a slow and very limited adoption of autologous endothelial cell seeding in clinical practice.

Keeping in mind the limitations in the current working procedure and the important lessons learned from past efforts to create an endothelial-lined synthetic graft, we asked ourselves if certain untested current technologies could be incorporated into the original

Mansfield-Herring one-stage approach. A practicable procedure was envisioned as one that would not significantly alter the current practice such that the surgeon needed special training, the patient required multiple procedures, or a hospital needed to add specialized facilities and staff. This procedure would also use a synthetic graft material (with or without minor modifications) with an established history of clinical use. In the end the approach must also clearly provide benefit and result in a statistically and clinically significant better outcome than the standard procedure. In the complex milieu of variables recognized to play a role in the successful development of an endothelial cell lining, we chose to focus our investigation on three main questions. First, is the graft material itself optimum to receive autologous cells in terms of known factors important to cell adhesion, growth, and the physical environment of flowing blood? The graft material used most frequently in cell seeding efforts has been ePTFE. This material presents a relatively smooth surface morphology of solid flat islands of PTFE (nodes) interlocked with a myriad of micron-thin fibrils (Figure 3). With cells in tissue culture known to prefer solid flat surfaces, the extent of this preferred morphology on ePTFE is limited to its fractured and thin nodal structures. In addition, adherence and retention of cells on the relatively non-contoured ePTFE surface is greatly challenged by eventual exposure to forces from flowing blood. To examine this question we investigate a modified ePTFE material, referred to as bePTFE [14], which presents a contoured surface morphology of both higher flat surface area for cell adhesion and 15-30 $\mu$ m recesses to help shield cells from flowing blood (Figure 3). The second question was: is a short static or slow-rotation deposition of cells adequate to distribute cells and allow a shear

resistant uptake on the graft surface? The early and the established clinical cell seeding procedures have utilized this approach, yet intuition and reports [15, 16] suggest that a substantial number of seeded cells simply become lost immediately following cross clamp release. With a host of alternative approaches involving certain applied forces to achieve a more even and adhesive interaction of cells on materials [17-20], we investigate here a simple and often-used approach to separate cells from fluids – g-force. To accomplish this we apply high g-force axial centrifugation to seed endothelial cells from suspension onto the graft surface. Since we are investigating the combination of an altered material and new cell seeding approach, the third area we focus on regards whether the presence of various proteins and/or hematologically-derived materials continues to be critical factor in cell seeding and subsequent cell growth. Investigators realized early on that endothelial cell uptake, growth, and retention is greatly facilitated using various materials derived from blood or presenting cell adhesive proteins [3, 5, 10, 15, 16, 21]. The mechanism of action behind these biological materials is thought to be through physical entrapment and/or specific recognition of binding domains on adhesion proteins and receptor proteins on the endothelial cell membrane. We therefore examined the utility of graft treatment with a number of commonly recognized cell-adhesive proteins to study their influence on uptake and growth of cells following g-force cell seeding. This effort includes treatment of graft materials with platelet poor plasma (PPP) generated from a bench top system designed for OR use to rapidly generate autologous PPP for wound care management. Finally, in order to efficiently identify significant factors and the variables to include in a pilot in vivo study on a practicable one-stage cell

seeding process, all in vitro and in vivo studies applied factorial experimental design approach.

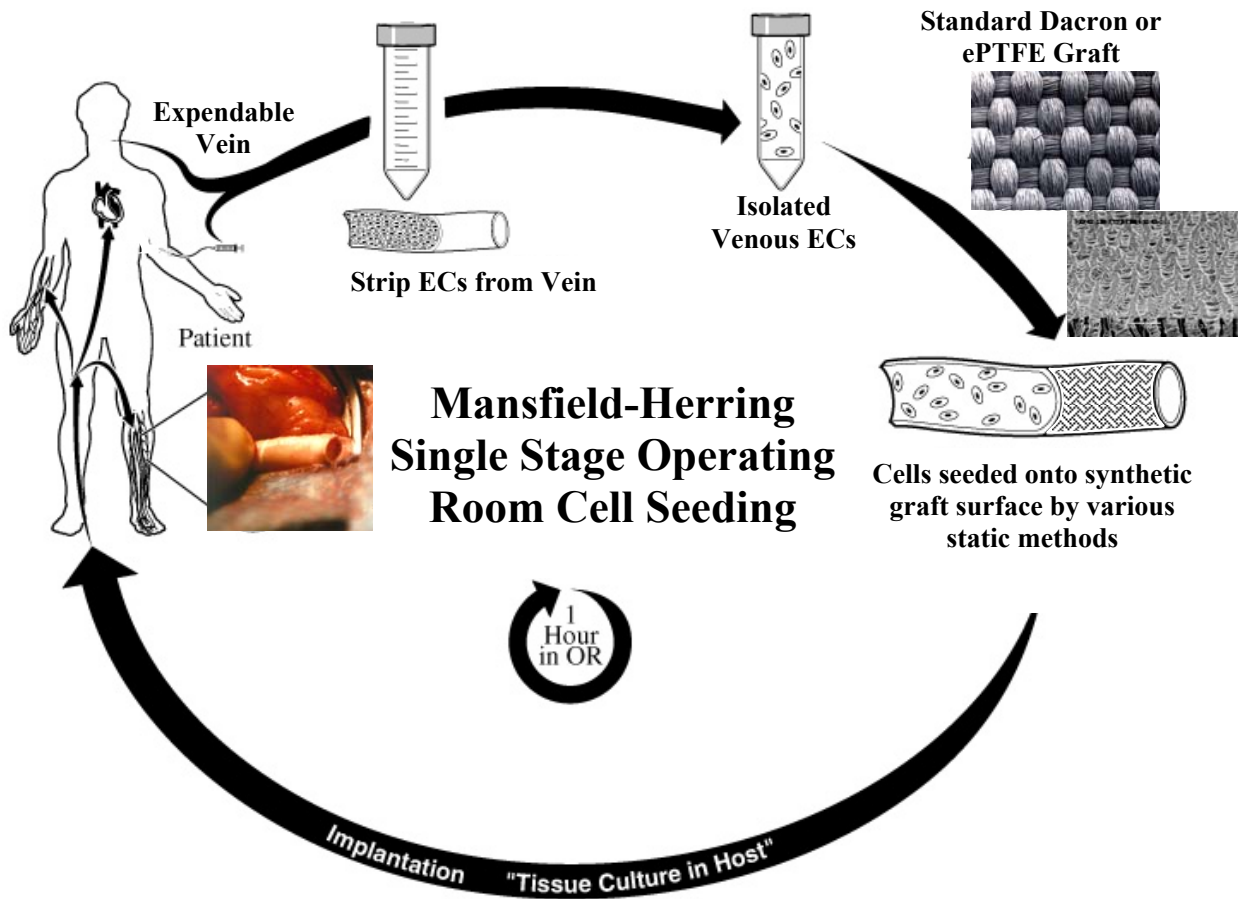


**Figure 1.** The Mansfield-Herring single-stage operating room vascular graft seeding procedure to apply venous endothelial cells to a vascular graft surface. The process takes approximately an additional hour in the operating room to complete.

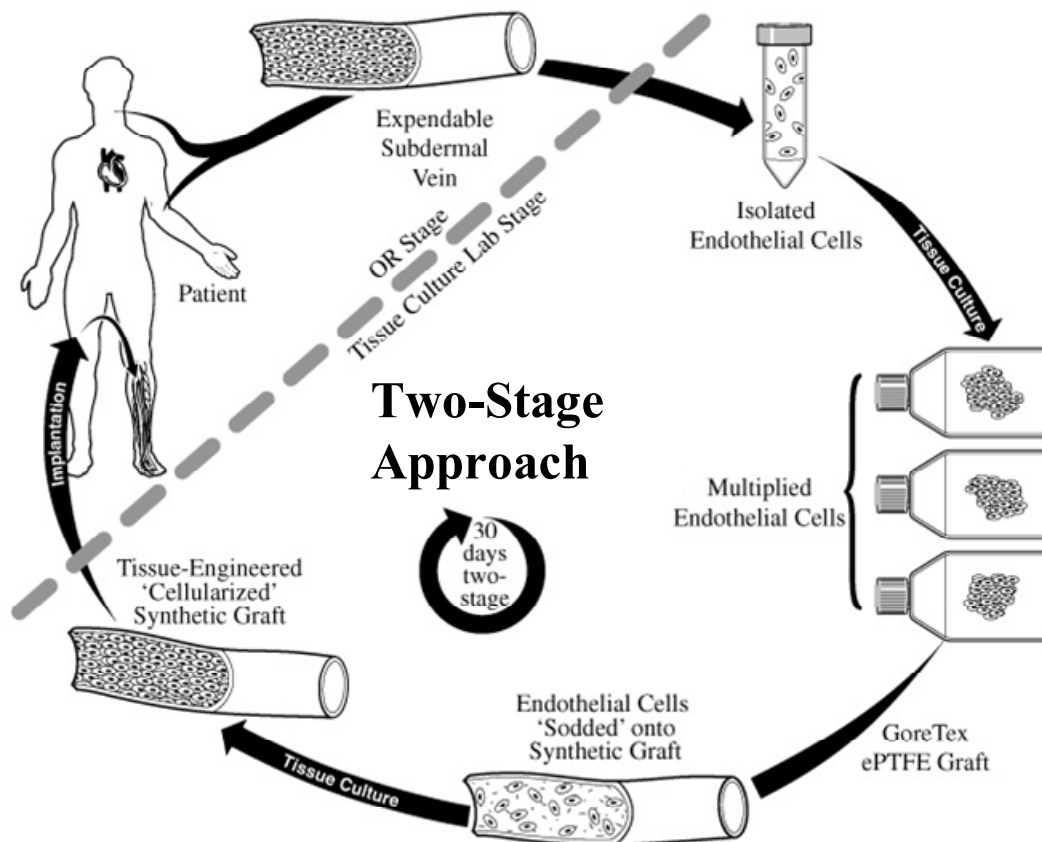


**Figure 2.** Schematic of the ‘two-stage’ approach to seeding a vascular graft with autologous endothelial cells. The operating room (OR) stage consists of two parts itself: vein harvesting and graft implantation 30 days later. The tissue culture lab stage consists of receiving the excised vein and stripping off and isolating the endothelial cells; expansion of the endothelial cells in culture; and seeding the cells on the graft followed by additional culturing to allow for cell acclimation and adhesion.



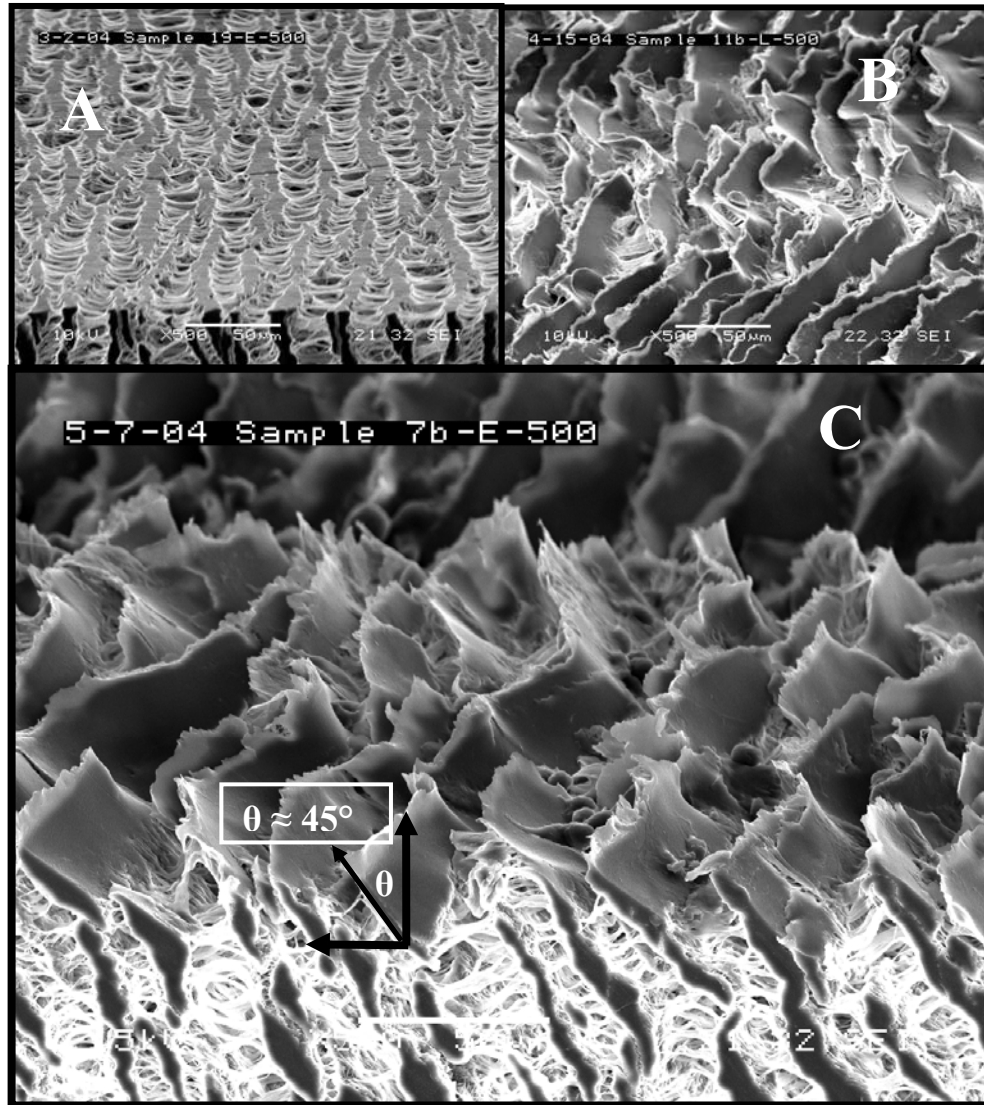


**Figure 3.** Scanning electron micrograph of standard ePTFE (A) and brushed ePTFE (bePTFE, B). The bePTFE shows distinct alteration in the luminal node geometry, with the nodes appearing to be elongated and oriented in a general outward direction with distinct spacing in between. C. bePTFE showing the directionality and approximate angular orientation of the modified PTFE nodes.

## MATERIALS and METHODS

**Expanded polytetrafluoroethylene (ePTFE) and brushed graft materials.** Clinical grade 4 mm ID (5.08 x 4.45 OD x ID (mm); 630  $\mu\text{m}$  wall thickness) ePTFE vascular graft materials (Bard Peripheral Vascular OEM Products, Model SN: AFAO5023, REF#: 50S04) with and without luminal surface modification were used throughout the studies. Luminal surface modification was applied using a physical brushing technique that altered the upper 15-30  $\mu\text{m}$  node-and-fibril structure. For this, nylon wheel brushes (Mill Rose, #71810) rotating at 1300 rpm were allowed to lightly touch the surface of 12-15 cm lengths of *everted* graft material mounted on a rectangular mandrel. The contact was carried out while the graft assembly traveled the direction of the longitudinal axis of the graft at a rate of approximately 12 mm/min. After all four sides were brushed and the mandrel removal, re-eversion allowed presentation of the physically-modified surface at the luminal aspect of the graft. This treatment transformed the classic node-and-fibrin surface architecture into one with regular lifted and smeared nodes of substantially altered surface texture and luminal surface area (Figure 3). The modified graft material, referred to as ‘brushed’ ePTFE (bePTFE), reveals 15-30  $\mu\text{m}$  deep luminal circumferential grooves and flanked by continuous smeared nodes separated by approximately the original internodal distance. The transformed nodes are oriented approximately 45° in the direction of brushing [14].

**Chemical and Physical Characterization.** Surface chemistry and bulk physical properties of the bePTFE material were tested for similarity to the original material. Contact angle measurement used the sessile-drop technique at room temperature and a Ramé-Hart A-100 goniometer equipped with a video measuring system. Samples were prepared by making a longitudinal slit on graft samples followed by fixation of the abluminal surface to glass slides using double-face tape (n=6 measurements per material). Electron spectroscopy for chemical analysis (ESCA) utilized a Physical Electronics Quantum 2000 Scanning ESCA to first generate survey spectra to determine all elements present (except H) on 200 micron spots of test samples (3 spots on 3 representative samples from each material). Spectra were then used to obtain quantitative surface composition by integrating the areas under the photoelectron peaks and applying empirical sensitivity factors. The X-ray source was monochromatic Al K $\alpha$ , the take-off angle was 45 degrees, and a charge correction F<sub>2</sub>-C-, in F1s spectra was set to 689.7eV. Physical characterization included mass per unit length gravimetric analysis of representative 1-cm lengths of relaxed materials. Also included were longitudinal and circumferential stress-strain analyses for modulus. This work utilized an MTS Sintech 1/D instrument (MTS Systems Corporation) equipped with a 50-pound load cell and cross head movement set to 50 mm per minute. Representative relaxed 7-cm and 1-cm sample lengths were used for each test, respectively (n = 2 and 3). Material porosity was estimated using a Gurley Model 4340N Automatic Densometer & Smoothness Tester set up to measure the time it takes for 300mL air to pass through 0.65 cm<sup>2</sup> of material at 31 mm H<sub>2</sub>O pressure. A Crescent Design Hydraulic Burst Leak Tester Model 250 was used

to determine the water entry pressure of the graft materials. The later tests were performed according to ISO 7198 [22].

**Cell preparations and seeding considerations.** In vitro cell seeding studies utilized endothelial cells from Clonetics™ aortic endothelial cell system kits. These kits contained cryo-preserved third-passage human aortic endothelia cells (HAECs) and media optimized for HAEC growth [Clonetics EGM-2 BulletKit (CC-3162)]. Supplier characterization of the HAEC included immunofluorescent staining for positive acetylated LDL and von Willebrand (Factor VIII) antigen and negative staining for smooth muscle  $\alpha$ -actin. For each study, HAECs were cultured to 80% confluence in separate 75 cm<sup>2</sup> plates. Cells were then combined and re-suspended to yield fresh suspensions of approximately  $1.0 \times 10^6$  cells/mL. A 450 $\mu$ L aliquot the cell suspension was placed into the lumen of 4 cm x 4 mm (L x ID) graft samples loaded into centrifuge tubes. Each test graft material was pre-fitted before and throughout experimentation with a light friction-fit external sleeve of thin-walled PTFE (Small Parts Inc.). The sleeve functioned to minimize potential for graft dehydration and handling artifact e.g., bending or compaction. The centrifuge tubes containing sleeve-covered grafts were then subjected to axial centrifugation at various conditions of g-force and time. A typical centrifugation consisted of 250g for 5 minutes at room temperature. The resulting seeding of 450-500 x 10<sup>3</sup> cells was estimated to be approximately 1/3 the confluent density of arterial endothelium. This was determined by approximating the fusiform endothelial cell ‘footprint’ to the geometry of an ellipse. Here the major (R) and minor (r) radii were

taken to be  $45\mu\text{m}$  and  $10\mu\text{m}$ , respectively (see Figure 4). This approach estimates a fully spread and confluent endothelial cell to present a surface area of  $A_{\text{EC}} = \pi rR = 353\mu\text{m}^2$ . Using the fixed luminal surface area of the test graft specimen gives approximately 1.5 million cells required for a sodding density. For the in vivo studies, a similar  $450\mu\text{L}$  aliquot of cells were used, with these cells consisting of an autologous venous endothelial suspension derived according to the methods described in Vein Harvesting and Cell Stripping.

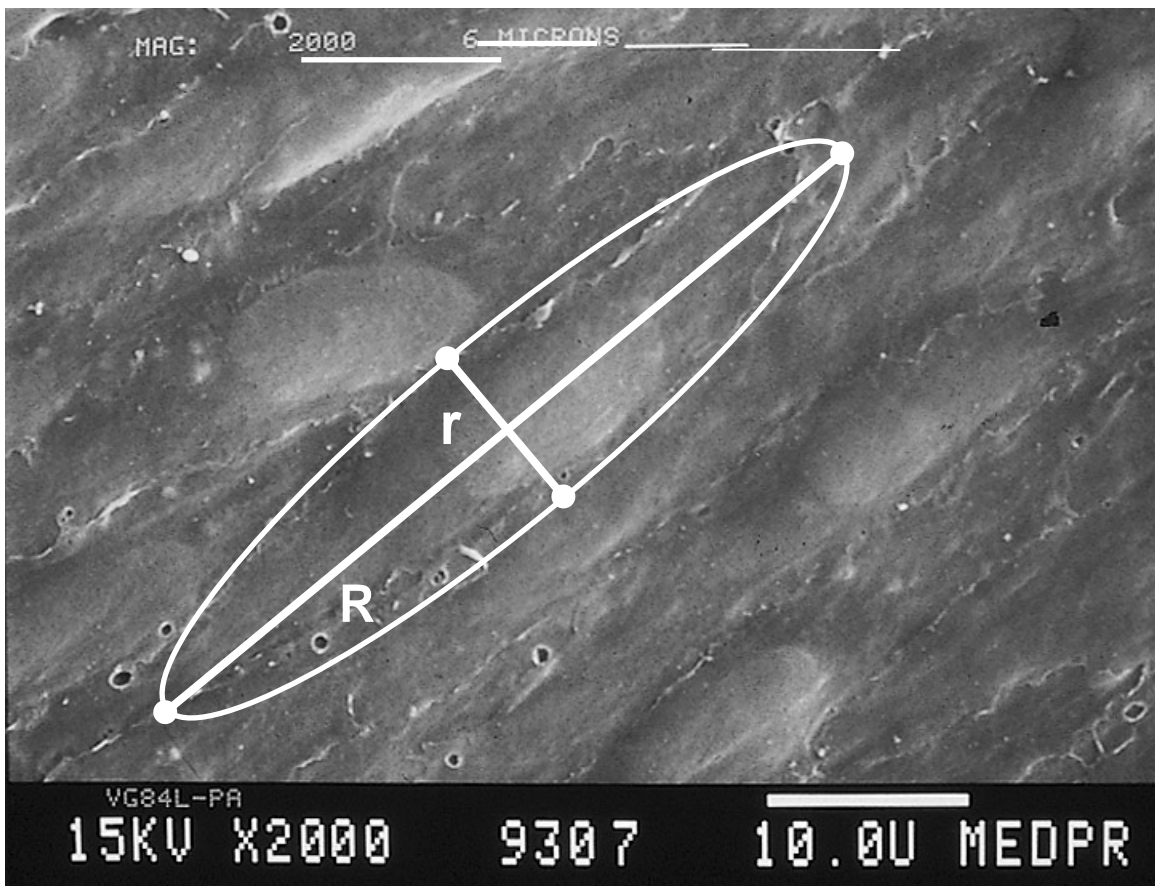


**Figure 4.** Scanning electron micrograph of arterial endothelium. The individual endothelial cell has a fusiform shape that approximates the geometry of an ellipse of major (R) and minor (r) axes of  $45\mu\text{m}$  and  $10\mu\text{m}$ , respectively.

**Design and principle of an axial centrifuge cell seeding system.** Cells of numerous types safely experience a wide range of handling and g-forces conditions in cell separation, isolation, and concentration processes used today. For this reason, g-force cell seeding was chosen as a rapid and safe manner to evenly distribute endothelial cells onto tubular graft surfaces. Using this approach, the relationship of g-force and rotational velocity (rpm) for a 4 mm ID graft rotated along its axis was determined from the formula for centripetal force,  $a = \omega^2 r$ . Here,  $\omega$  is the angular velocity in radians per second and  $r_g$  is the internal radius of the graft (in units of meters). To determine actual g-force,  $\omega$  is replaced with  $(\text{rpm}2\pi/60)$  and the resultant centripetal force,  $a$ , is divided by the acceleration of gravity at the surface of the Earth ( $9.8 \text{ m/s}^2$ ). Thus, g-force on cells at the graft wall,  $g_w$ , was determined by:  $g_w = [(\text{rpm}2\pi/60)^2 r_g]/9.8$ . G-forces of 50, 250, and 500g, forces commonly used in cell separation processes, were targeted for the investigations. Here, a '1g' condition consisted of a 1 rpm rotation of test samples in centrifuge tubes using a standard bench top tube rotation system (Cole Parmer Roto-Torque Model 7637). To apply the high axial rpm required to achieve the high g-forces, an Eppendorf 5416 centrifuge and fixed angle rotor (Type 16 F 24-11) were used. The rotor required modification with a highly-balanced centrally-mounted assembly fixed to the rotor surface. This assembly allowed axial positioning of a custom-made polycarbonate centrifuge tube containing one 4 cm long 4 mm ID graft with an external PTFE sleeve. For efficient experimentation using factorial experimental design, four such systems (Figure 5) were constructed to allow experimentation in replicas of up to 4.

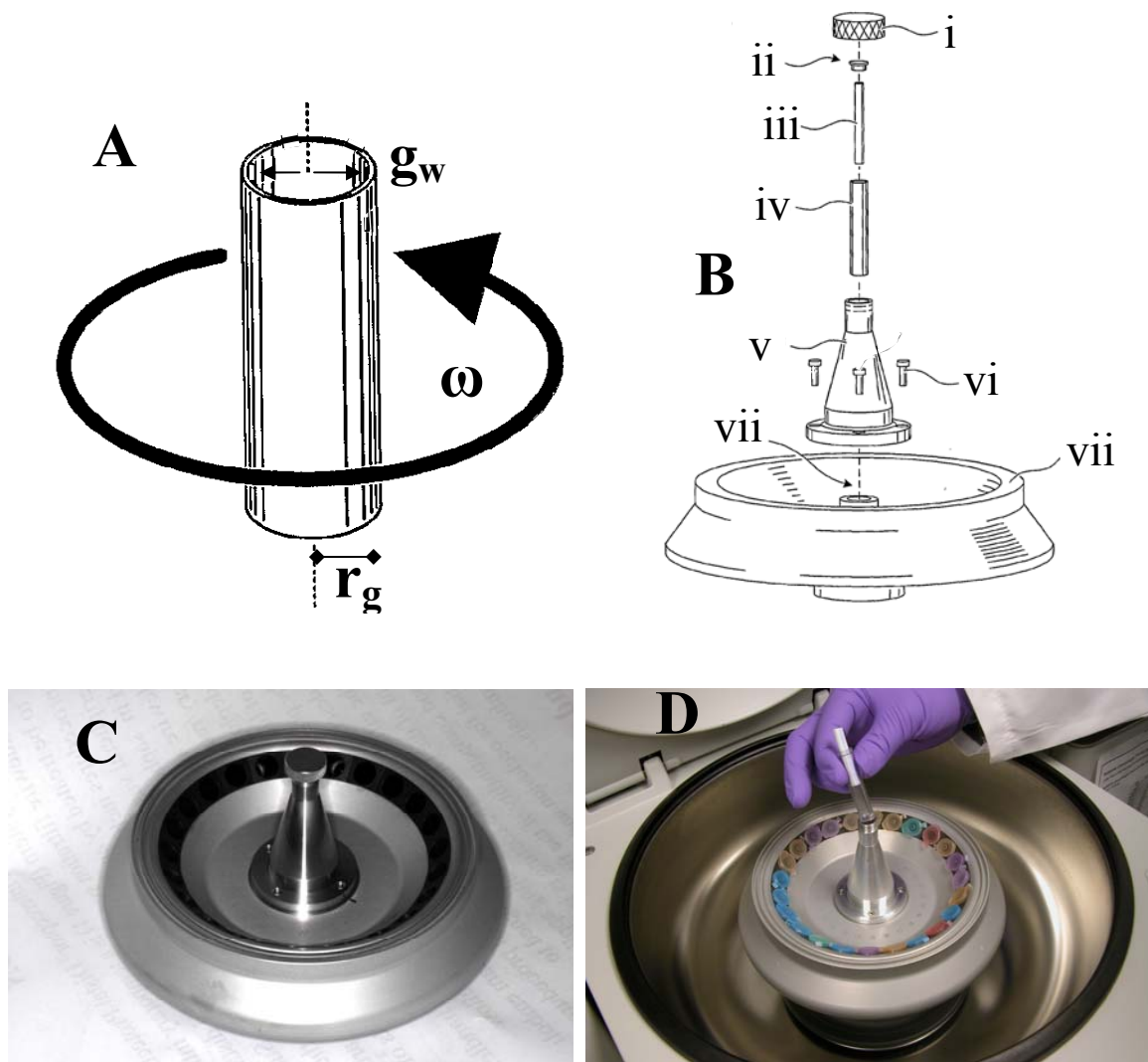


**Figure 5.** Axial rotation of the tubular vascular graft under high speed rotation while filled with a suspension of endothelial cells allows rapid and even distribution of endothelial cells along the graft luminal surface. A: The cells experience g-forces at the wall ( $g_w$ ) according to  $g_w = [(rpm \cdot 2 \pi / 60)^2 r_g] / 9.8$ .  $r_g$  = internal radius of the tubular graft,  $\omega$  = angular velocity. B: Modified rotor components: i. rotor cap, ii. centrifuge tube cap, iii. graft, iv. centrifuge tube, v. axial cone centrifuge tube/graft holder, vi. mounting screws, vii. mounting apparatus that affixes rotor to centrifuge, viii. original fixed-angle rotor base. C: Photograph of modified rotor. D: Axial centrifuge system with modified rotor in centrifuge.

**Cell uptake and cell viability assessment.** Enumeration of viable cells that were seeded onto the ePTFE graft surface was estimated using the CellTiter-Glo™ luminescent assay (CTG, Promega, Madison WI) which measures live cell ATP levels. The ePTFE graft samples were cut into 5 mm pieces using a precision sectioning block and fine razor blades, and sections were placed into an opaque 96-well plate. The CTG assay was performed per instructions. Here, the number of cells was determined by comparing ATP levels to those of standard curve of known cell numbers. In addition to the CTG assay, the distribution of live and dead cells were observed using the Live/Dead® cell Viability Assay (Invitrogen, Carlsbad, CA)

**In vitro studies to identify influential factors in endothelial cell uptake/seeding on graft materials.** Variables identified to have a potential impact on the efficiency and viability of g-force seeding of endothelial cells were: material type (M), g-force level (GF), centrifugation time (CT; 15 vs. 60 minutes), number of centrifugation runs (CR; 1 vs. a second run following gentle cell resuspension in the graft), incubation time (IT; 0 to 60 minute incubation post centrifugation), graft hydration (H; non-hydrated vs. hydration with culture media), presence of serum in media (S), number of cells (#C; 450 vs. 900 x 10<sup>3</sup>), and post seeding exposure to pulsatile flow (F; no flow vs. 1 hour pulsatile flow). For the flow studies, a modified version of the computer-controlled microstepping motor system previously described [23] was used. Here, the programmable rotational motion system, geared for 20,000 steps per 360° revolution, was used to impart a 60 beat per minute (1 Hz) motion to stacked tissue culture plates placed in an incubator (Figure 6).



The seeded graft specimens in their protective PTFE sleeves were mounted in the outer edge of 150 x 15 mm tissue culture plates using sterile technique and sterile suture tape (Steri-Strips, 3M). Application of a 200 ms sigmoidal acceleration curve followed by an 800 ms pause was estimated to produce physiological shear forces and 50 and 250 ml/minute average and peak flow of tissue culture fluid through the graft tubes. Graft hydration was accomplished by degassing samples in 200-proof molecular biology grade ethanol followed by hydration in EBM-2 (Cambrex; CC-3156) culture media in three sequential 15-minute incubations in fresh media. Application of g-forces was as described above.

The identified factors were studied in a series of simple factorial experimental design studies (Figure 7). For example, one design consisted of a 2x2x2 factorial study on g-force (0 vs. 250g), time of exposure to cells (5 vs. 10 minutes), and material type (ePTFE vs. bePTFE). These experiments were focused at determining the conditions most favorable for cell uptake and cell viability. All materials consisted of 40 mm x 4 mm (L x ID) ePTFE or bePTFE graft materials. Experiments involved materials exposed to  $450 \times 10^3$  cells in 450  $\mu$ L under each described condition. After graft materials were exposed to the specified conditions, grafts were sectioned into equal 5 mm segments. End segments were discarded and the middle segments were randomly assigned to analysis by CellTiter-Glo™ luminescent assay, Live/Dead® Cell Viability assay, and/or SEM for visual appearance. ANOVA analyses on luminescent assay data was used to determine which factors had the most significant impact on cell uptake ( $P < 0.05$ ).

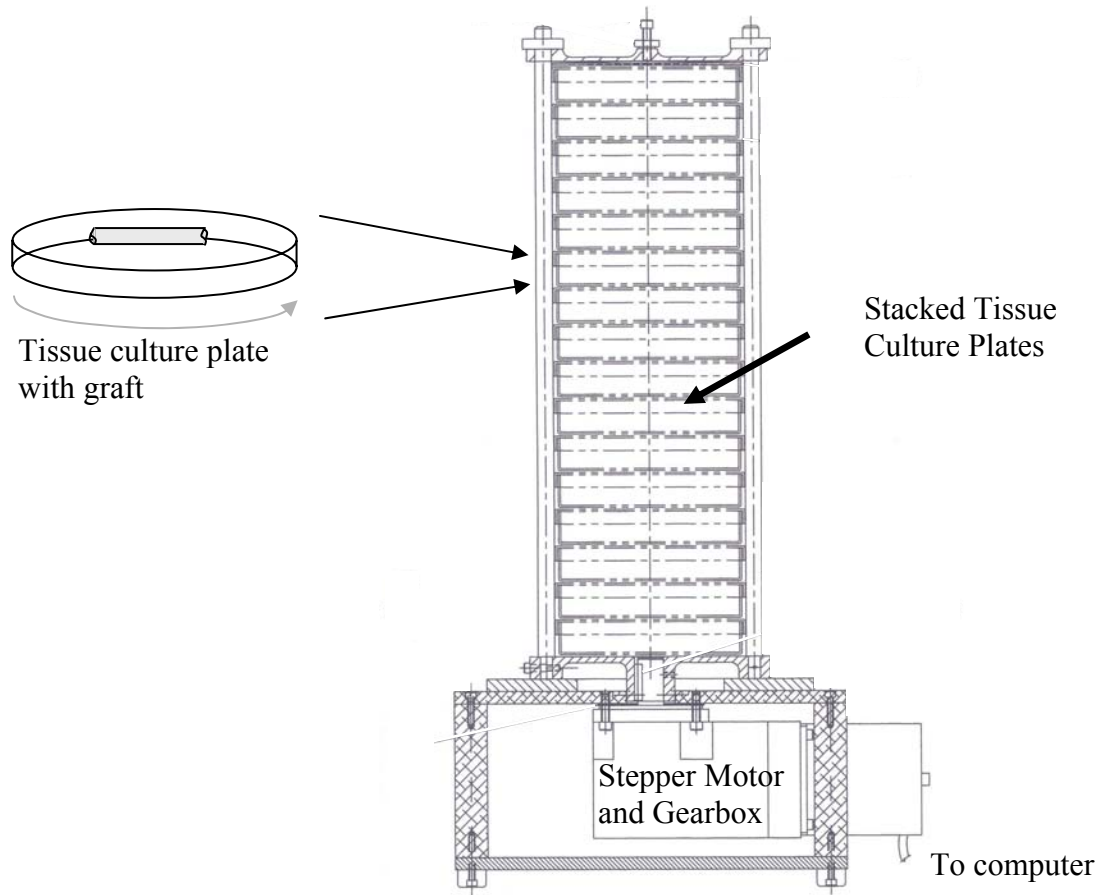


**Figure 6.** In vitro pulsatile flow tissue culture model. The stacked tissue culture plates undergo a specific rotational pattern allowing tissue culture to flow through graft specimens in a pulsatile fashion.

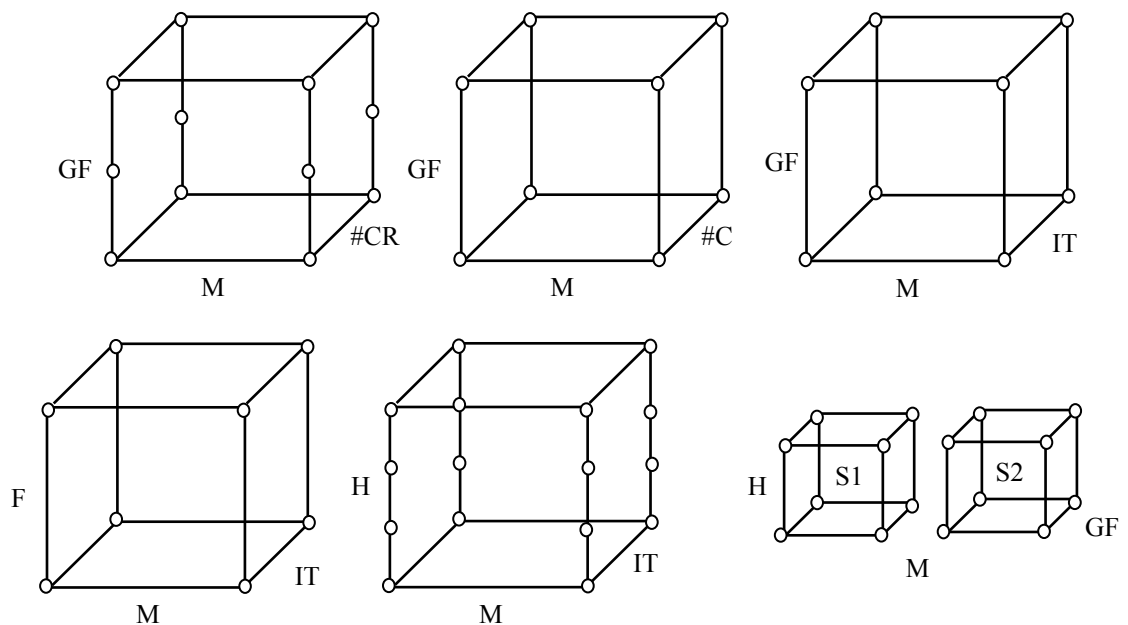


**Figure 7.** Representative study designs for characterizing and optimizing uptake of ECs on graft surfaces under various conditions

**In vitro cell culture studies to identify graft pre-seeding treatments that support endothelial cell growth.** Recognizing that cell uptake alone on bare graft material may not be conducive to cell growth, a number of graft material pretreatments were examined for impact on endothelial cell growth following seeding. Treatments examined were: hydration (H, as described above) and hydration followed by luminal exposure for 30-60 minutes to fresh platelet-poor-plasma (PPP). The latter was generated using healthy drug-refraining human donors and a Magellan™ operating room centrifuge (Medtronic Magellan™ Platelet Separator, Medtronic Inc.). Fresh PPP was allowed to incubate in the refrigerator for 1-24 hours to allow settling of the red blood cell component. Anticoagulation consisted of a 1:9 ratio of sodium citrate to whole blood. Additional treatments were: 60 min incubation in fibronectin (Sigma); 60 min incubation in Matrigel™ (BD Biosciences); and 60 min incubation in BSA (Hyclone). The materials

labeled PPP1, PPP2, and PPP3 represented PPP applied before cell seeding, after cell seeding, and concomitantly with cell seeding, respectively. All graft materials were hydrated with EBM-2 media, as described, before exposure to the test treatments. Cells were cultured on the pretreated grafts for 5 days using standard procedure followed by CTG analysis for cell enumeration.

**Vein harvest, autologous endothelial cell stripping, and simulated OR cell seeding.**

This methodology was done in accordance with current clinical cell seeding methods [6,7,9]. Briefly, the lateral saphenous vein was removed following no touch dissection, in situ cannulation, and careful ligation of all side-branches. Cannulation used a vessel cannula (Medtronic #30004) and attached 1-way stopcock (Cole Parmer #30600-00). Ligation utilized small and medium titanium ligating hemoclips (Weck Closure Systems, 523835 and 523680) and standard Prolene suture as needed. The vein was flushed clear of blood using 37°C HBSS solution followed by introduction of 0.1% collagenase (Sigma C6885) in HBSS media. After 15 min 37°C incubation, the collagenase cell suspension was collected and neutralized with 10% autologous serum. The cell suspension was centrifuged and brought up in 500µL EBM-2MV (Cambrex) media. This suspension was used for graft seeding following removal of 50 µL for cell count assay. This approach was chosen following a 3x2 factorial experimental design study on vein source (cephalic vs. femoral vs. lateral saphenous) vs. harvesting method (cannulation vs. vein eversion). The cannulation method isolates the stripping enzyme to the vein interior and the eversion method submerses the everted vein in the enzymatic solution. This cell harvesting study was concomitantly used to conduct mock OR cell seeding on the test

and control materials. To gain experience in OR seeding, and to measure the extent of cell harvest variation, the later study was completed using  $n = 4$  on each condition (four canines/8 veins of each type = 24 veins).

**In vivo graft implantation study.** A canine bilateral interpositional femoral artery replacement model was employed. The study design (see below and Figure 8) called for the use of 16 animals and 32 graft implants. Briefly, 4.0-cm lengths of test and control graft material were implanted contralaterally using end-to-end anastomoses and two lengths of uninterrupted 7-0 Prolene running 180 degrees around each anastomosis. Animals received aspirin (325 mg SID) and dipyridamole (25 mg BID) through the length of the study. Cell-seeded and unseeded grafts were brought to the OR table each in a protective PTFE removable sleeve that aided in prevention of dehydration and crushing during surgery. After completing the proximal anastomoses the sleeve was removed and discarded. A GE Vivid 7 Ultrasound was used to record femoral artery blood flow before and after graft implantation, and at 2, 4, and 6 weeks (termination). Animals were euthanized at six weeks followed by physiological-pressure lower extremity perfusion fixation using buffer and 2.5% glutaraldehyde. This study was performed in accordance with the Federal Good Laboratory Practices (21 CFR Part 58) under the approval of the Animal Care and Use Committee at Medtronic Inc.

**In vivo study design.** The in vivo portion of this work consisted of a full factorial ( $2^4$ ) experimental design on the following four variables: Material (ePTFE vs. bePTFE),

material Direction (bePTFE with nodes oriented with flow vs. against flow – see Figure 3), platelet poor plasma (PPP) pre-treatment (none vs. with PPP), and EC Seeding (no seeding vs. seeding). See Figure 8. All conditions were done in duplicate. For technical reasons, restricted randomization was applied such that (1) all animals received an ePTFE graft and a bePTFE graft, and (2) surgeries on the first eight subjects involved only non-seeded grafts i.e., the second eight animals received all seeded grafts. For added control, sham vein harvesting was included on the first eight subjects. The later enabled operating room staff to also run mock vein stripping and cell seeding procedures prior to the actual seeding cases. Grafts were randomly assigned to the right and left positions. Animals were allowed to recover for 6 weeks with ultrasound assessments of graft patency at 2, 4, and 6 weeks. To avoid confounding endothelium arising from seeded cells with endothelium derived from anastomotic endothelial outgrowth, grafts were allowed to mature for only 6 weeks in vivo. Previous studies using the same animal model showed midgraft endothelium generally absent in similar length ePTFE grafts at this time point. Animals were euthanized at 6 weeks and examined using gross pathology, histopathology, and SEM analysis.

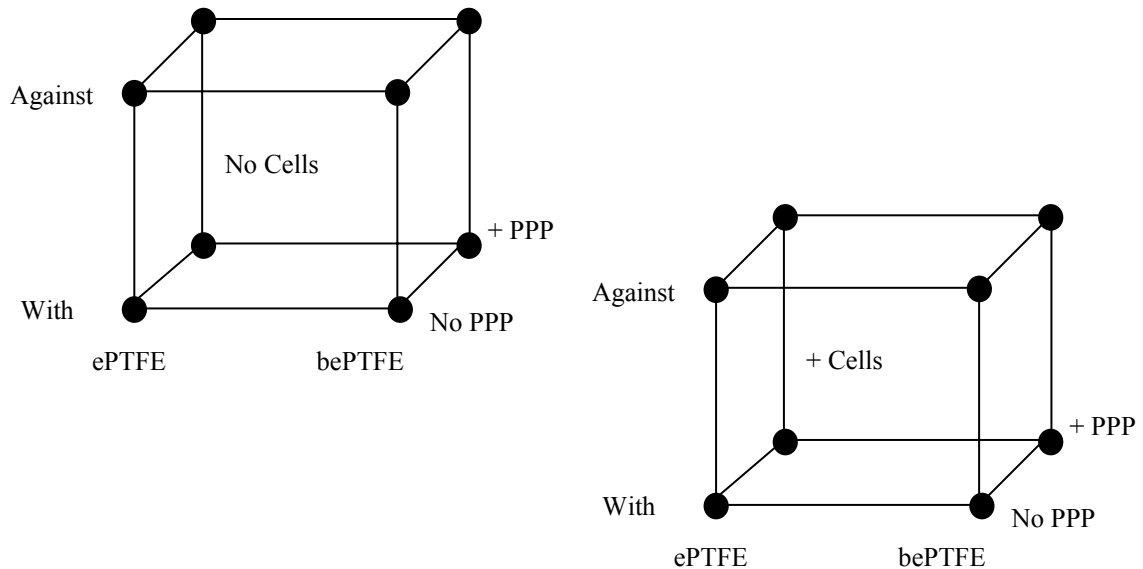


**Figure 8.** Geometric representation of the in vivo factorial experimental design. The study consisted of a  $2^4$  full factorial on Material (ePTFE vs. bePTFE), PPP treatment (with PPP vs. without PPP), Orientation (bePTFE nodes directed towards vs. against blood flow), and g-force cell seeding of endothelial cells (with cells vs. without cells). PPP = platelet poor plasma, '+' = with, '-' = without.

**Gross and histopathology assessments.** Grafts were removed en bloc following euthanasia and lower extremity perfusion fixation. Photographs were taken at low and high magnification of midgraft and anastomotic regions before and after longitudinal hemisectioning. Grafts were scored for apparent red deposits/resolving surface thrombus in blinded fashion by two of the authors according to the scale: 0 = none, 1 = 0-25%, 2 = 25-50%, 3 = 50-75%, 4 = 75-100% and 5 = 100%. One complete hemisection was designated for SEM analysis and the other for standard histology. Samples for SEM analysis were placed in 2.5% buffered glutaraldehyde and samples for histology were stored in 10% buffered formalin. Standard paraffin-embedded histology included

staining with H&E, Masson's Trichrome, PTAH, and Von Gieson stains. Histological assessment was evaluated based on the following main categories and simple scoring system: thrombosis, neointima formation (apparent coverage by endothelium), anastomotic hyperplasia, overall graft cellularity (cellular component within the interstices of the porous PTFE), and macrophage infiltration (inflammatory response). Scoring by the study pathologist consisted of the following categories: 0 = no minimal level of response observed; 1 = minimal response observed; 2 = intermediate level of response observed; 3 = high level of response observed. Due to overlap and linkage of the inflammatory response, normal wound healing, and thrombotic events that occur at the key graft regions i.e., at anastomoses, within the graft interstices, at the lumen, and at the periadventitial surface, only the middle sections were utilized for statistical analysis.

**Scanning electron microscopy (SEM) assessment of endothelial seeding and**

**coverage.** In vitro seeded graft materials, cell-stripped veins, and graft explants received primary fixation in 2.5% buffered glutaraldehyde and secondary fixation in 1% osmium tetroxide followed by dehydration in graded ethanol solutions. Specimens were then critical point dried and sputter-coated with gold. SEM evaluation was performed using a JEOL 5910 Low Vacuum SEM at 10 - 15 kV, 20-50x magnification. Due to the size of each graft, approximately 20-40 individual images were montaged into one large image using Adobe Photoshop®. In PowerPoint software, lines were placed along the graft from proximal to distal anastomoses to render 10 equal segments. Segments 1-3 and 8-10 were defined as regions likely to be occupied by endothelium from anastomotic



outgrowth. Segments 4-7 were defined as mid-graft regions where endothelial presence was considered indicative of cells derived from the seeding process. Extent of endothelialization in each segment was assessed using three representative high magnification (200X) SEM images taken within each segment. The following scale was used by four of the authors to blindly score the extent of endothelial surface area coverage: 0 = none, 1 = 0-25%, 2 = 25-50%, 3 = 50-75%, 4 = 75-100% and 5 = 100%. This same scale was applied to evaluate the efficiency of cell stripping on veins.

**Statistical Analyses.** Statistical work up consisted of ANOVA analysis on numerical data (CTG luminometer data) and numerical scores (SEM scores of vein surfaces and explant graft surfaces, and histology scores on explanted vascular grafts). Data was analyzed using DesignEase Software. The data underwent the standard General Factorial ANOVA analysis of each measured response. Significant responses were those with  $P < 0.05$ . Graphical representation of some data includes means diamonds in which the width of the diamond represents the samples size and the horizontal line represents the group mean. In cases of comparison of pairs of responses, a two-tailed Student's t-test was performed. Given the small samples size and the binomial measurement, analysis of study variables against patency data utilized SAS 9.1 statistical software and the proc-logistic procedure combined with the exact option.

## RESULTS

### **Graft Material Characterization.**

#### Surface Topography

The physical brushing of standard ePTFE involving control of brush rpm, contact duration, normal force, and direction, resulted in a topographical modification affecting the upper 15-30 $\mu$  of the luminal surface. Figure 3 shows scanning electron micrograph images of standard ePTFE and brushed ePTFE (bePTFE) revealing the lifting and smearing impact of the brushing process. The modified topography presents a higher solid PTFE surface area arranged in a wave-like fashion, with 15-30 $\mu$  recesses flanked by thin solid PTFE tilted at an approximate 45° angle.

#### Surface Chemistry and Physical Properties

The surface chemistry of the ePTFE and bePTFE materials was characterized by contact angle measurements and ESCA to check for similar surface tension and chemistry presentation at the blood- and endothelial cell-contacting surface. Contact angle data indicated the expected hydrophobic nature of the fluorinated hydrocarbon with no statistical difference in water contact angle measurement between ePTFE and bePTFE (Table 1). For the ESCA analysis, the theoretical concentrations of C and F for PTFE are

33% and 67%. Only C and F were detected on all areas of standard ePTFE, and their relative concentrations are close to the expected values for PTFE. High resolution XPS performed on the C1s and F1s photoelectron peaks showed a gaussian C1s peak with binding energy of 292.5eV (representative of CF<sub>2</sub> species), which was referenced to an F1s peak binding energy of 689.7eV. This is consistent with PTFE. For the representative bePTFE samples, similar results were obtained. A trace amount of oxygen of unknown origin was detected at its detection limit in one sample identified as a sample taken from the end of a length of material. This was an area of higher level of handling.

The ePTFE and bePTFE graft materials were also tested for consistency in physical properties using a sampling of standard tests frequently applied to tubular vascular prosthesis [22]. The tests performed included longitudinal and circumferential stress strain analysis, water entry pressure testing, and air permeability testing. The water entry pressure data indicated that the altered luminal surface geometry did not significantly impact water permeability into the material. However, stress strain data did indicate an approximate 20% decrease in both longitudinal and circumferential modulus. In addition, air permeability testing indicated significantly higher air permeability in the bePTFE material. These findings suggest that the handling e.g., eversion and re-eversion and/or the brushing itself results in a slight loss of strength and increase in permeability to the ePTFE material (Table 1). The surgeons conducting the in vivo portion of this report noted no difference in the handling and suturability in the two graft materials. The gravimetric analysis on linear mass density (mg/cm) on the two materials was not found

to be statistically significant (data not shown). However, this data is believed to be confounded by untracked subtle lot-to-lot variation in ePTFE that overrides any potential change in mass due to the modification process.

**Table 1.** Graft Material Chemical and Physical Properties

<b>Test</b>		<b>ePTFE</b>	<b>bePTFE</b>
<b>Contact Angle (°)</b>		140 ± 5	133 ± 9
	<b>% C</b>	31.6 ± 0.2	31.6 ± 0.1
<b>ESCA</b>	<b>% O</b>	0	0.1 ± 0.1
	<b>% F</b>	68.4 ± 0.2	68.3 ± 0.1
<b>Circumferential Modulus (Mpa)</b>		4.04 ± 0.14*	3.14 ± 0.07*
<b>Longitudinal Modulus (MPa)</b>		173.1 ± 2.5*	141.7 ± 9.5*
<b>Water Entry Pressure (kPa)</b>		50.1 ± 0.4	52.4 ± 3.6
<b>Gurley Air Permeability (s)</b>		710 ± 106*	526 ± 10

\* Difference between groups determined to be statistically significant by Student’s paired t-test (P<0.05)

### **Axial Centrifugation Cell Seeding**

A rapid and even seeding of endothelial cells on the vascular grafts was achieved using the modified rotor centrifuge system to impart axial centrifugation on grafts containing cell suspensions (Figure 5). Target g-forces of 50, 250, and 500g were precisely obtained using the system set at 4726, 10569, and 14947 rpm. The modified rotor remained balanced throughout all runs and speeds. The added hardware on the rotor precluded attachment of the original protective cover for the rotor, making operation noisy due to wind turbulence over the fixed angle openings. Noise was mitigated by adding blank 1.5 mL conical tubes to the exposed fixed angle tube slots. While the system allowed centrifugation of only one sample at a time, the multivariable factorial experimental designs and technical details became manageable using four axial centrifuge systems in

the tissue culture suite. The protective centrifuge lid was the limiting factor for the height of the rotor modification and therefore the length of test graft specimens studied.

### **In vitro studies for factors influential to endothelial cell uptake/seeding and growth**

ANOVA analyses on the in vitro factorial experimental design studies identified the following factors as having a consistent significant ( $P < 0.05$ ) impact on the uptake or retention of endothelial cells on the graft materials: type of graft material, g-force, graft hydration, incubation time post centrifugation, and post seeding exposure to pulsatile flow (Figure 9). Regardless of material type, the uptake of endothelial cells appears to plateau between 50 and 250g (Figure 9A). Gentle rotation at 1g lead to little cell uptake regardless of material type, whereas 50g and 250g exposure showed significant material uptake of cells, with bePTFE material consistently showing higher levels (Figure 9B). Having the graft material prehydrated with culture media before g-force seeding with cells appeared to be important to achieve high cell uptake on standard ePTFE, yet the bePTFE material showed high uptake regardless of state of hydration (Figure 9C). In experiments to compare cell retention under pulsatile flow conditions, both ePTFE and bePTFE showed retention of seeded cells under flow condition, with the bePTFE again showing higher overall levels of cell uptake (Figure 9D). Allowing cells to acclimate 15-60 minutes following g-force seeding produced a minor increase in retained cells. Exposure to extended centrifugation, a second centrifugation run, and the seeding density did not have a significant impact on the uptake of endothelial cells. In subsequent five-

day tissue culture studies on graft pre-seeding treatments intended to support the growth of cells after seeding, Table 2 shows that seeded cells following PPP treatment was associated with the greatest significant ( $P < 0.05$ ) cell growth. All other treatments, besides some growth on Matrigel™, showed a loss of cells over this time period.

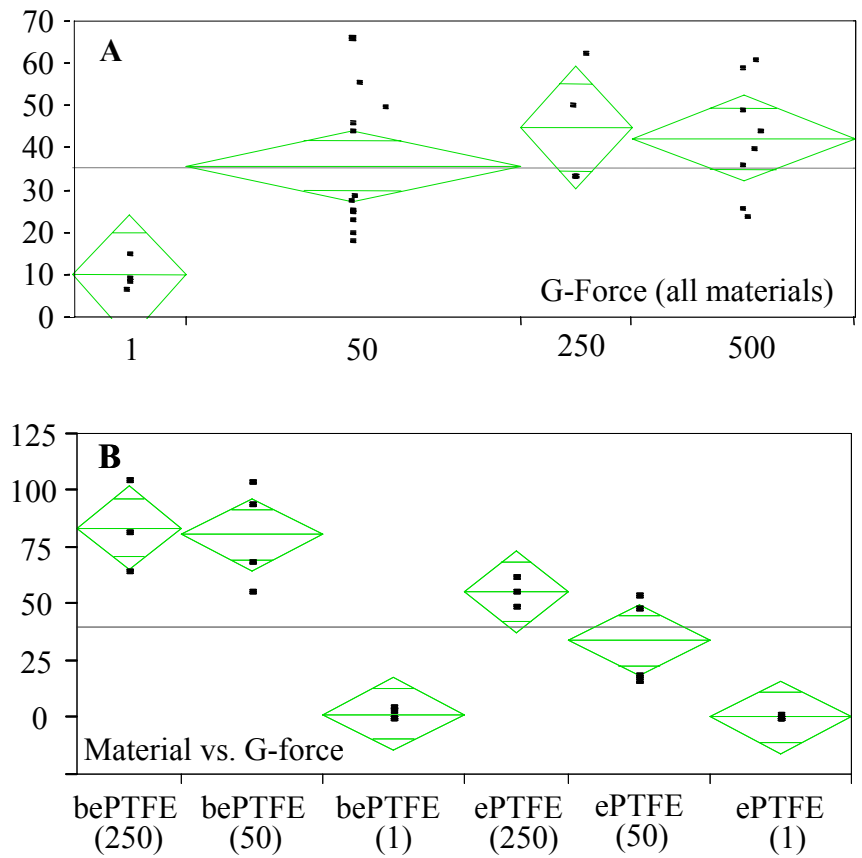


**Figure 9.** Effect of g-force applied in axial centrifugation cell seeding on uptake of endothelial cells on graft materials over a broad range of experimental conditions (A), and by specific graft material and g-force (B). Y-axis = % uptake of applied endothelial cells. *Continued on next page.*

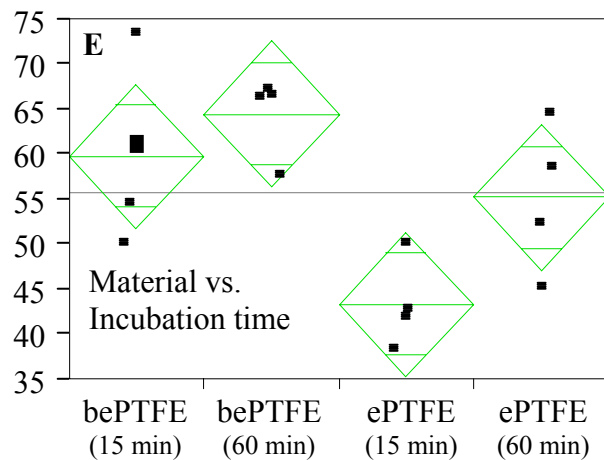
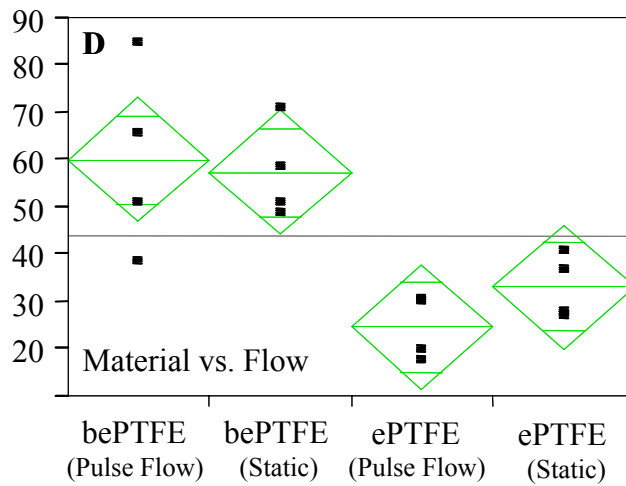
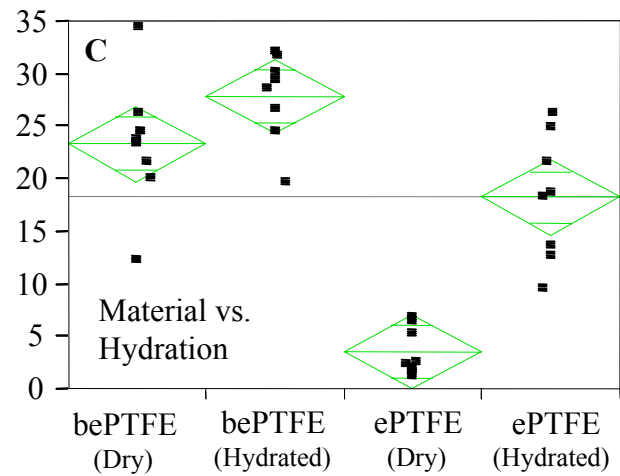


**Figure 9 (continued).** C: Effect of graft hydration on uptake of endothelial cells applied by axial centrifugation cell seeding. D: Impact of pulsatile flow following seeding. E: Influence of incubation immediately following seeding by axial centrifugation. Y-axis = % uptake of applied endothelial cells.

**Table 2.** Factorial experimental design studies for endothelial cell (EC) growth on synthetic graft materials containing various pretreatments and g-force seeded ECs.

Study	Variables (Design)	Graft Pre-Treatment	Cell Growth (% gain/loss)
1	M, IT (2x3)	None	-57% to -96% loss
2	M, IT (3x3)	None	-69% to -98% loss
3	M, IT, H (2x2x2)	Hydration Only	-69% to -95% loss
4	M, IT, GPT (2x2x3)	None, Serum, FN	-32% to -91% loss
5	M, IT, GPT (2x2x2)	None, FN	-56% to -95% loss
6	M, IT, GPT (2x2x3)	PPP1, PPP2, PPP3	+7.3% to +564% gain
7	M, IT, GPT (2x2x2)	None, Matrigel	-89% to +37% loss/gain

The design variables tested included: material (M); Incubation Time (IT); and Graft Hydration (H). Other abbreviations are fibronectin (FN) and platelet poor plasma (PPP). Assessment of cell growth was done using the CellTiter Glo™ (CTG) assay described. Graft pre-treatments labeled PPP1, PPP2, and PPP3 represented PPP applied before cell seeding, after cell seeding, and concomitantly with cell seeding, respectively. The PPP1 treatment was associated with the highest growth of cells.

### **In vivo vein harvesting, endothelial cell stripping, and mock OR seeding.**

Comparison of numbers of cells acquired from endothelial cell harvesting on different canine veins using two different stripping methods is shown in Figure 10. The cannulation method, which mimics the clinically used procedures [5, 7], resulted in a statistically significant higher yield of endothelial cells compared to the vein eversion method. The anatomical source of the vein did not have a significant impact on number of harvested endothelial cells per surface area of vein removed. However, vein



dimension i.e., length and outer diameter, was clearly anatomically dependent, yielding:  $111 \pm 15 \times 4 \pm 1$ ,  $61 \pm 14 \times 7 \pm 2$ , and  $111 \pm 17 \times 5 \pm 0$  for the cephalic, femoral, and saphenous veins, respectively (L x OD, mm). With either method, the outcome was highly variable, with the cannulation and eversion methods retrieving 10-40 and 3-30 thousand cells per luminal square centimeter of vein, respectively. This figure is much lower than the theoretical density seen in vessels (Figure 4). This degree of variation was also reflected in SEM micrographs of the stripped veins (Figure 11). Here, some veins appear completely stripped of venous endothelium (Figure 11E) while others appear only partially denuded (Figures 11A-C). Some venous tissue even revealed large areas lacking any cell removal (10D). Live/Dead staining of graft materials that underwent mock OR cell seeding also showed a fair degree of variability (Figure 12). Generally, cells appear as both single and multicellular islands with fairly even distribution and survival. It was noticeable, however, for cells to aggregate in microscopic longitudinal grooves on the bePTFE surface (Figure 12C). These grooves result from the brushing process in which some bristles are of uneven height. SEM images revealed g-force seeded endothelial cells to typically rest in the PTFE fibril region of each material (Figure 13). The bePTFE material shows cells to often be located between the uplifted nodes (Figure 13D). The fibrinous surface that results from the PPP pre-seeding treatment appeared variable in density and degree of matting, and tended to mask visualization of seeded cells (Figure 13E-F).

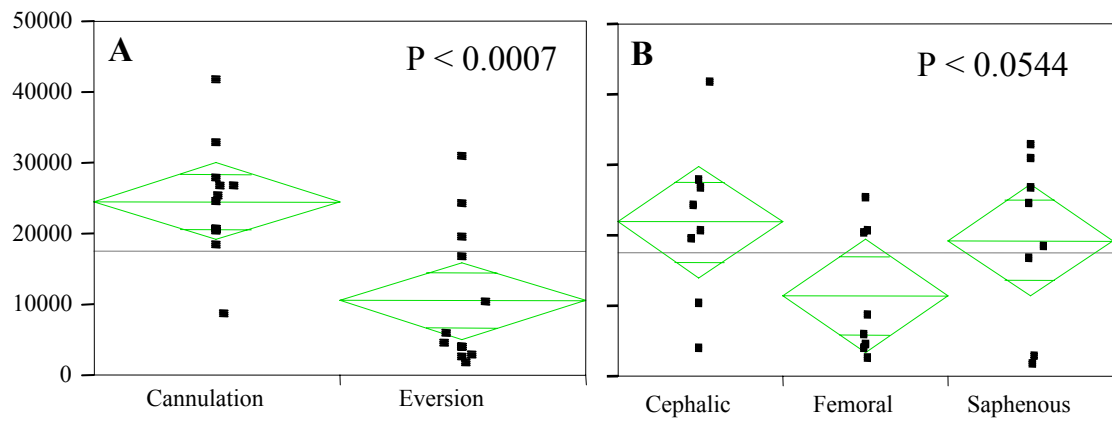
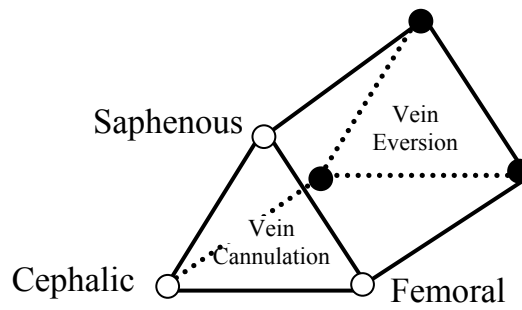


**Figure 10.** Cells per square centimeter venous tissue harvested by method (A) and vein source (B). The geometric representation of the factorial experimental design is shown above.

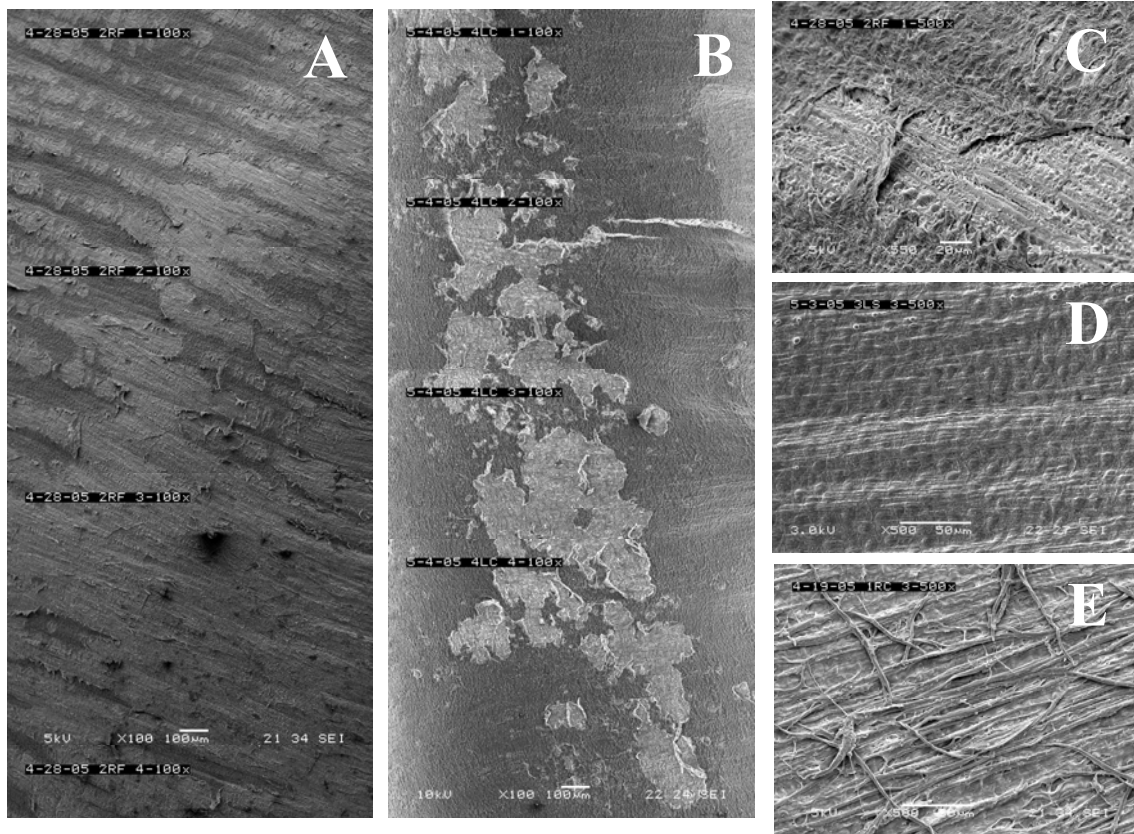


**Figure 11.** Representative 100X and 500X scanning electron micrographs showing the variation in enzymatic cell removal. A: Right femoral vein (montage), eversion method B: Left cephalic vein (montage), cannula method. C: Right femoral vein, eversion method. D: Left saphenous vein, cannula method. E: Right cephalic vein, eversion method. Note that montages of the extreme cases shown in D and E often revealed the majority of the surface with the same appearance.

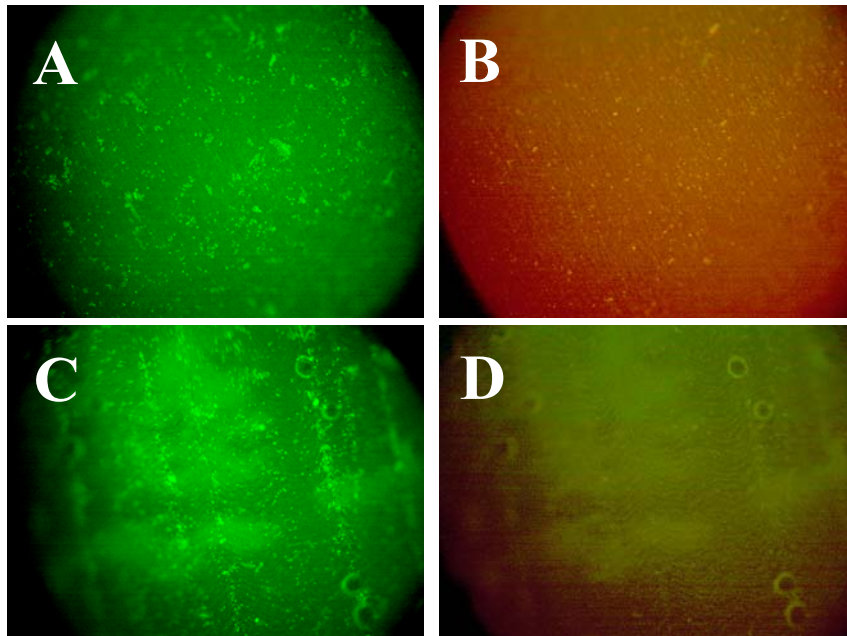


**Figure 12.** Representative Live/Dead assay of graft materials receiving PPP treatment and g-force seeding of canine venous endothelial cells. The images show stained endothelial cells on ePTFE (top row) and bePTFE (bottom row). A, C: GFP stain (green) depicts live cells. B, D: TRITC stain (red) depicts dead cells. The GFP and TRITC samples involved ECs obtained using the cannulation method. The lines in C represent endothelial cells tending to aggregate in microscopic longitudinal groves resulting from the brushing process.

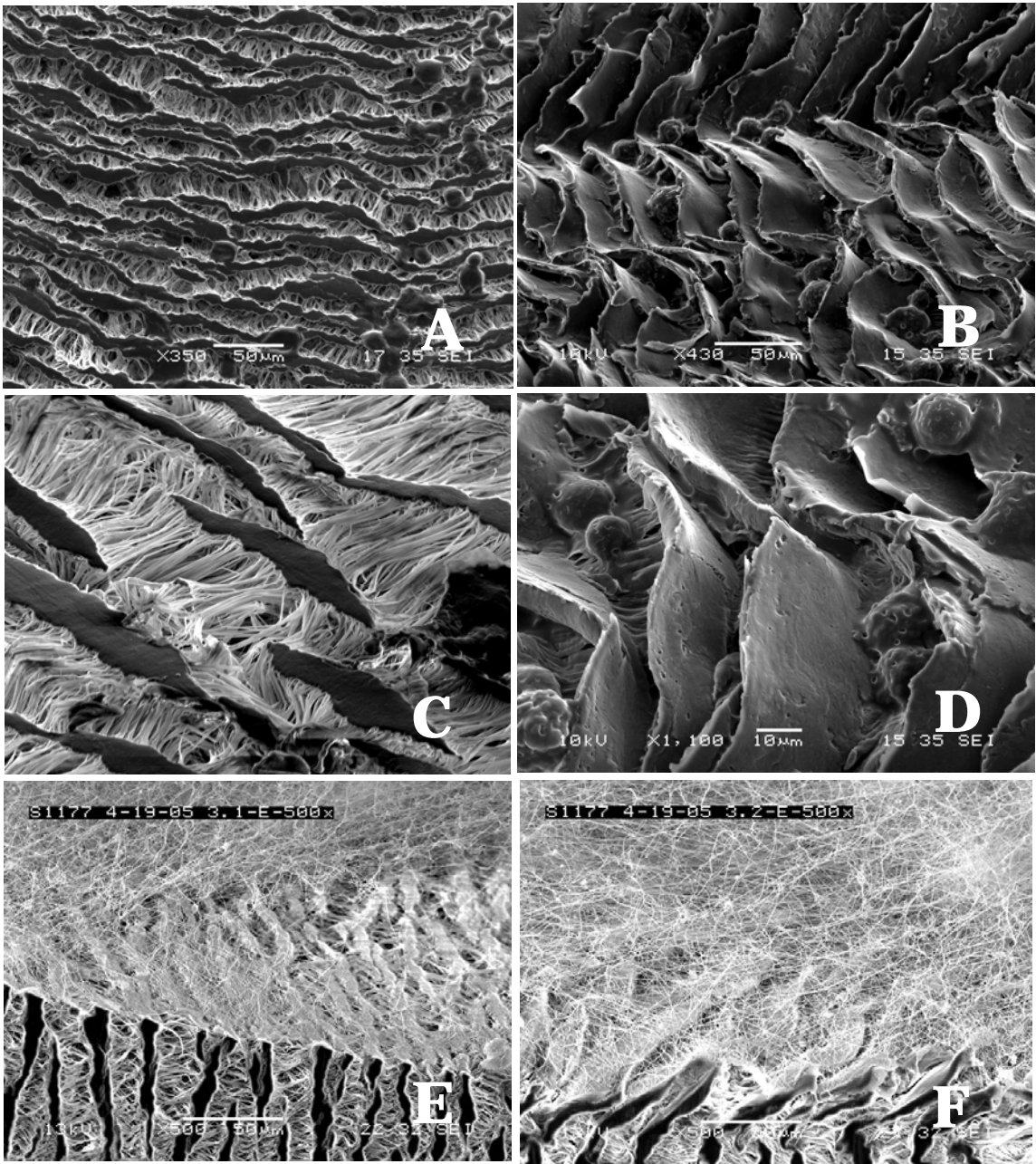


**Figure 13.** Scanning electron micrographs at two magnifications of ePTFE (A, C) and bePTFE (B, D) following axial centrifugation cell seeding. E and F are images of ePTFE and bePTFE surfaces following exposure to platelet poor plasma (PPP) and formation of an autologous fibrin platelet poor layer (aFPPL).

## **In vivo graft implantation study**

### Gross and histological observations

Table 3 summarizes graft patency data for the 32 vascular grafts implanted in the study. Overall, 10/16 of ePTFE grafts were patent and 14/16 bePTFE graft were patent. Statistical analysis of the main study factors against graft patency revealed no factors having a significant impact. Factors coming close to a statistically significant impact were material ( $P < 0.07$ ) and cell seeding ( $P < 0.08$ ). From general gross inspection, grafts appeared well healed by the 6 week implant duration with two animals showing bilateral graft occlusion, 4 animals showing unilateral graft occlusion (all ePTFE grafts), and the remainder showing bilaterally patent grafts. The cases of bilateral graft occlusion were identified to be associated with infection. ANOVA analysis on scoring of the visual extent of red discoloration at the surface yielded material, cell seeding, and PPP treatment to each have a significant ( $P < 0.05$ ) impact on the observation. Here, it was generally bePTFE grafts, cell seeded grafts, and PPP treated grafts that revealed less of the observation. A caveat on this particular observation is that not all red deposits were carefully scrutinized for consistency with active thrombosis. Representative gross images of patent grafts are shown in Figure 14.

**TABLE 3.** Graft Patency Data

<b>ePTFE Vascular Grafts</b>			
<b>Without Cell Seeding</b>		<b>With Cell Seeding</b>	
<b>- PPP</b>	<b>+ PPP</b>	<b>- PPP</b>	<b>+ PPP</b>
3/4*	3/4*	2/4	2/4
Total grafts patent: 10/16			
<b>bePTFE Vascular Grafts</b>			
<b>Without Cell Seeding</b>		<b>With Cell Seeding</b>	
<b>- PPP</b>	<b>+ PPP</b>	<b>- PPP</b>	<b>+ PPP</b>
3/4*	3/4*	4/4	4/4
Total grafts patent: 14/16			

\* Graft occlusions in these study animals were bilateral with suspected infection noted in the pathology reports

**Table 3.** Summary of graft patencies observed in the in vivo implant study. (Explanation: 3/4 signifies that 3 out of 4 grafts in this category were patent and one was occluded).

ANOVA analysis on the histological scores revealed that seeding with endothelial cells was the only factor demonstrating a significant impact on the histological response categories. Here, cell seeding was seen to have a significant impact ( $P < 0.05$ ) on extent of neointimal formation, overall material cellularity, and macrophage infiltration. In each case a higher level of each response was associated with the implants that received the cell seeding procedure. For the categories of thrombosis, acute and chronic inflammation, and anastomotic hyperplasia, none of the study factors appeared to have a significant influence. However, it may be noteworthy that the thrombosis and cellularity scores showed marginal dependence on the type of graft material present ( $P < 0.08$  [bePTFE, less thrombus], and  $P < 0.09$  [bePTFE, more cellularity], respectively). Figure

15 shows representative histological images taken at the midgraft region of patent grafts. The histological images generally reveal that regardless of type of graft, grafts without PPP treatment or cell seeding reveal a barren non-cellular midgraft. Grafts that received either PPP treatment alone or in combination with cell seeding reveal a thin cellular lining consistent with endothelium.

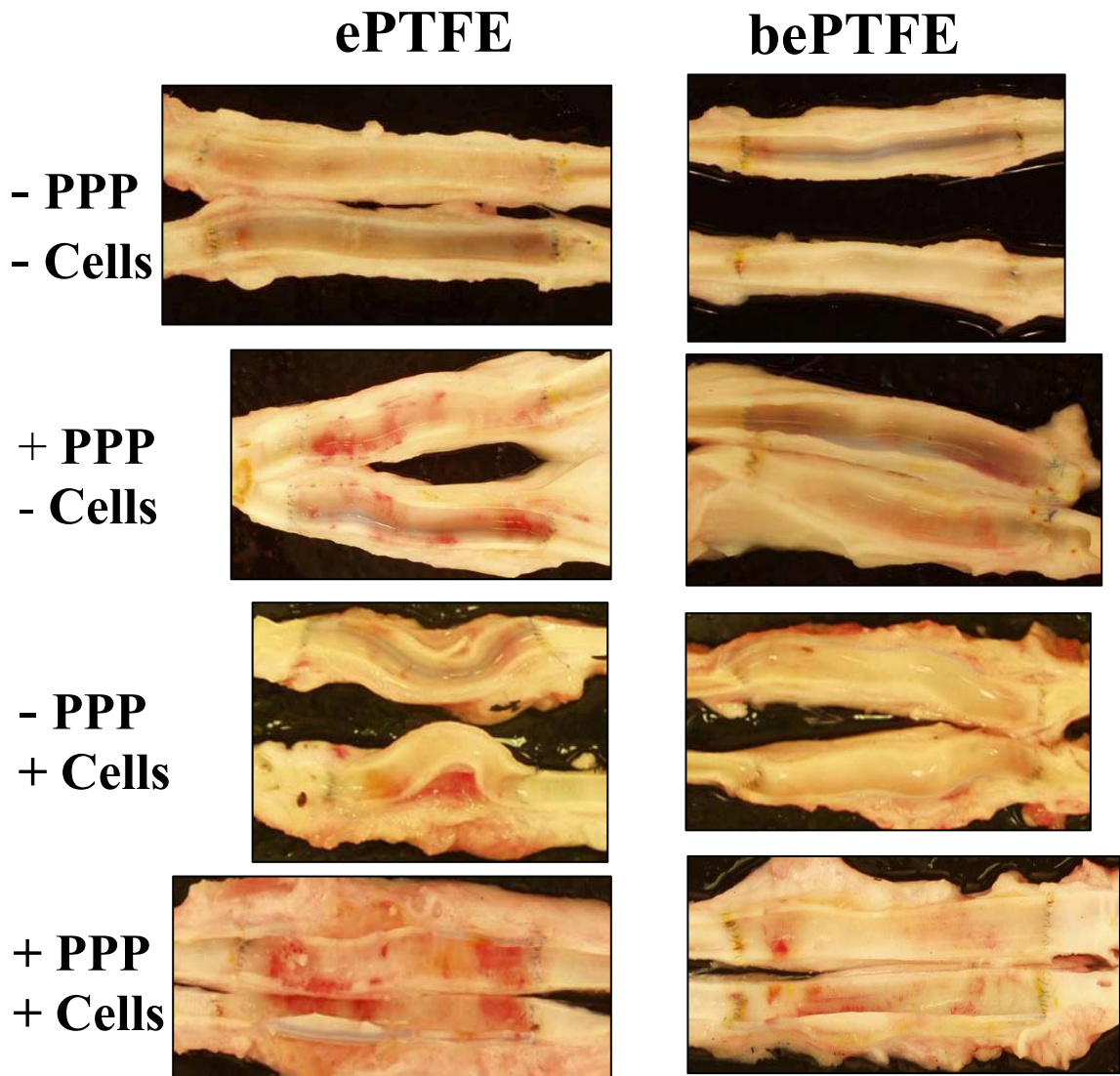


**Figure 14.** Representative gross photographic images of patent grafts each main test category. Symbols are: “-“ = without, “+” = with, PPP = treatment platelet poor plasma, and Cells = seeding lateral saphenous vein endothelial cells.



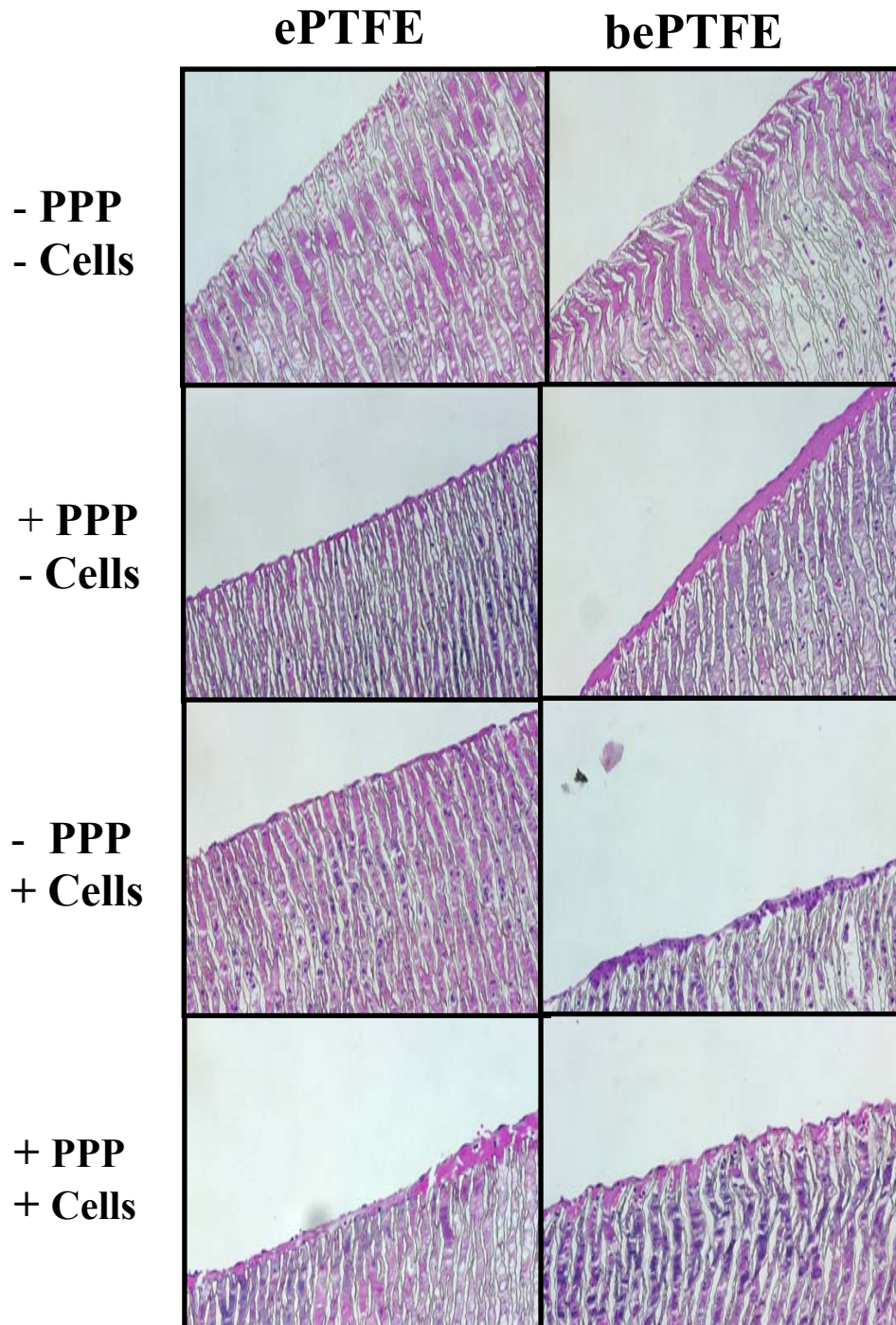


**Figure 15.** Representative H&E histology sections taken at the midgraft region of patent ePTFE and bePTFE vascular grafts. PPP denotes graft treatment with platelet poor plasma prior to cell seeding; 'Cells' denotes g-force seeding with autologous venous endothelial cells; '+' and '-' indicate with and without.

## Scanning electron microscopy observations

The goal of the in vivo portion of this report was to assess the impact of the study parameters on the extent of graft endothelialization. For this assessment, a montage of low magnification micrographs was first taken along an entire longitudinal hemisection of each patent implant. Three representative high magnification SEM micrographs were then taken in ten evenly divided segments from proximal to distal anastomosis to confirm the presence of apparent endothelium. A representative SEM montage of one graft explant and the segmenting scheme is shown in Figure 16. In this example, the montage and the 200X images reveal the typical extensive endothelialization noted on either graft material treated with PPP alone, treatment with cell seeding alone, or, treatment with PPP followed by cell seeding. Figure 17 reveals representative 200X images taken in the vicinity of regions 5 and 6 in each treatment group. As can be seen, most surfaces show a similar degree of endothelialization except in the control groups, which reveal primarily a noncellular surface. The average SEM score along each implant type is shown in Figure 18, where distinction between the two graft materials has been excluded given the lack of statistical significance observed with the material factor. Here, the ePTFE and bePTFE control grafts (no treatment with PPP or cell seeding) reveal that anastomotic endothelial outgrowth occurred to approximately one centimeter, and that minimal to no midgraft endothelialization was present at 6 weeks. Figure 18 also confirms that the order of apparent endothelialization in the midgraft regions was  $+Cells+PPP \geq +Cell-PPP \approx -Cells+PPP > -Cells-PPP$ . ANOVA analysis on the scores revealed that the factors

presenting a significant impact on the extent of endothelialization were cell seeding and PPP treatment.

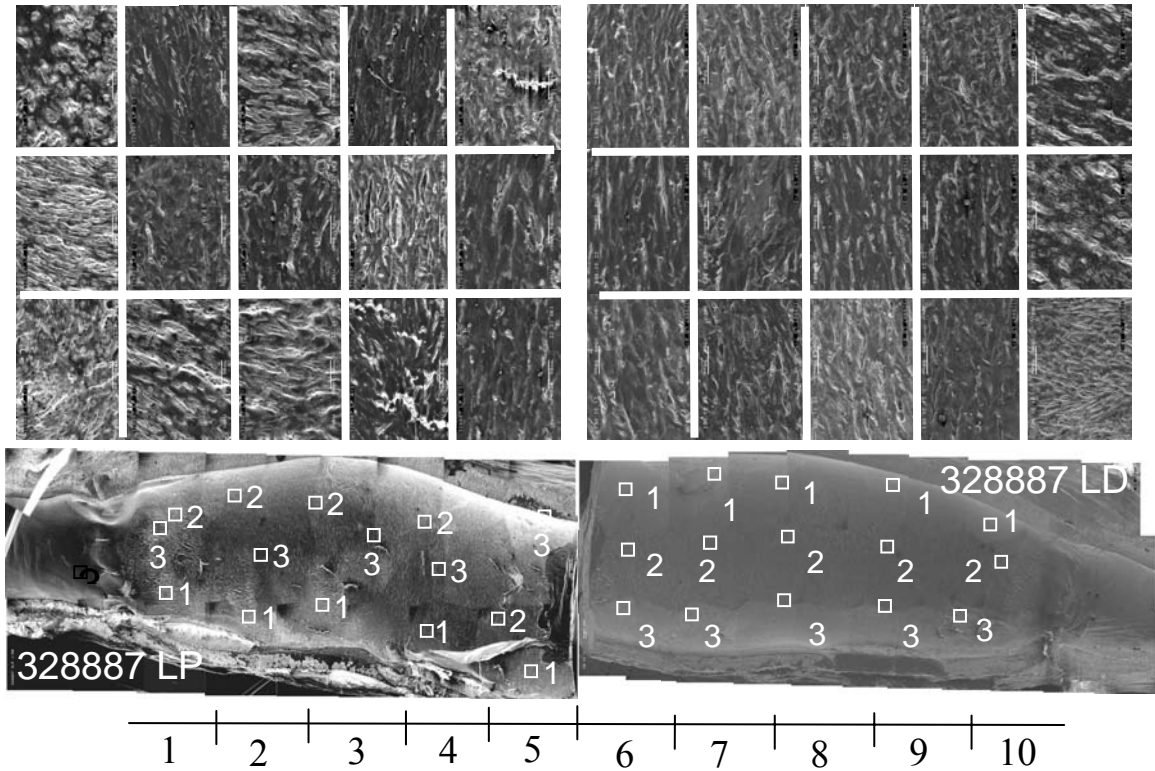


**Figure 16.** A representative low magnification SEM montage showing a complete graft hemisection and the location of three higher magnification 200X images (shown above) used to assess extent of endothelialization. The graft shown above is an ePTFE graft that received axial centrifugation cell seeding in the absence of PPP treatment.

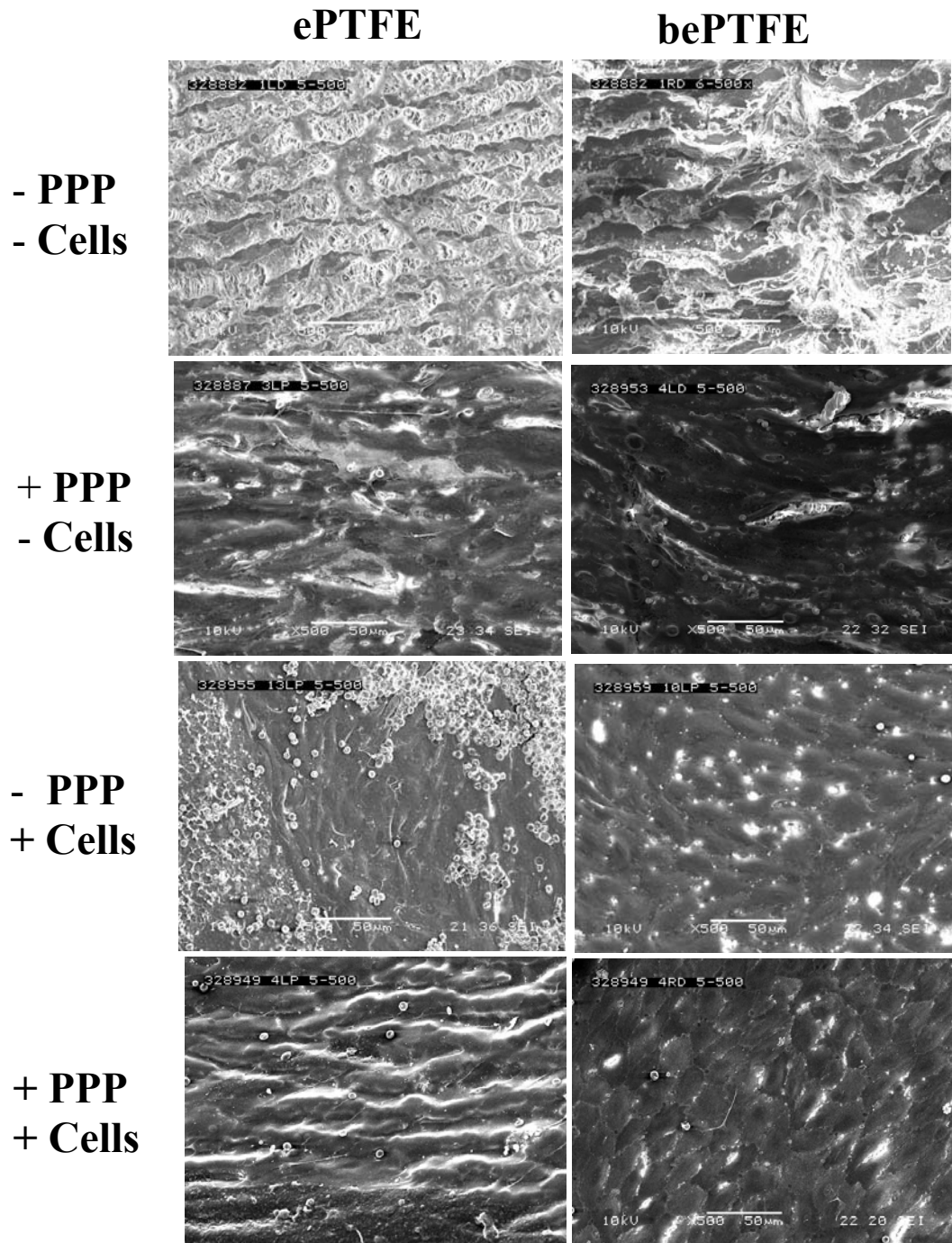


**Figure 17.** Representative SEM micrographs taken at the midgraft region of patent ePTFE and bePTFE vascular grafts. PPP denotes graft treatment with platelet poor plasma prior to cell seeding; ‘Cells’ denotes g-force seeding with autologous venous endothelial cells; ‘+’ and ‘-’ indicate with and without.

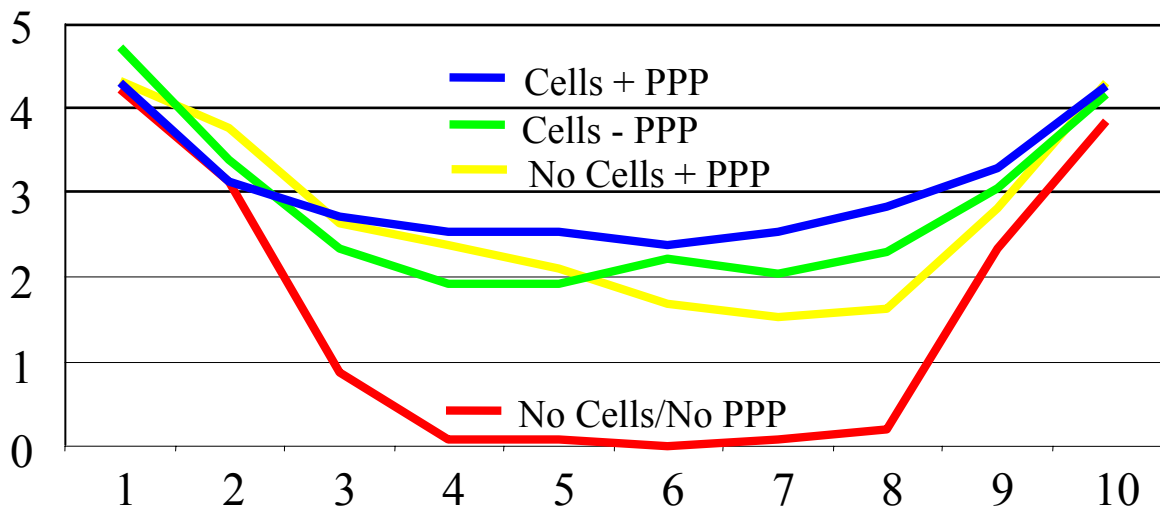


**Figure 18.** Graphical summary of SEM scores by treatment group and along the entire length of patent grafts. Note that graft type has been excluded and averages represent both ePTFE and bePTFE grafts in each group. PPP denotes graft treatment with platelet poor plasma prior to cell seeding; ‘Cells’ denotes g-force seeding with autologous venous endothelial cells; ‘+’ and ‘-’ indicate with and without.

## DISCUSSION and CONCLUSIONS

The goal of this research was to examine if certain new technologies might have a favorable impact on the originally-proposed one-stage OR process for seeding vascular grafts with endothelial cells. When Mansfield and Herring first suggested this approach three decades ago, it was the cell that was recognized to be the basic unit of biological function. During the ensuing years of effort to apply endothelial cells to grafts, advances in cell and molecular biology established that homeostatic cell function was not significantly dictated by the cell alone. Rather, the unit of function was widened to include the significant influence of the extracellular environment. This interaction of the cell with its environment has been described as a *dynamic reciprocity* of complex

physical, chemical, and molecular interactions that act in concert to maintain normal cell and tissue function [24]. In the context of a change in extracellular environment, the removal of endothelial cells from the vein, their subsequent placement onto a synthetic graft material, and their re-introduction to an arterial environment represents a significant perturbation from their normal extracellular surroundings. It is not surprising then that this perturbation, and the extent of cell recovery in adaptation to a new microenvironment, has been a key factor in variation in cell seeding results observed over the years. Surely, factors in methodology and variation in results has hindered the standardization of a general procedure for endothelial cell seeding.

Towards minimizing this variation, and in attempt to make a more simple procedure, we first examined the graft material itself and wondered if a physical alteration might improve uptake and retention of endothelial cells. For this we looked at a modified version of ePTFE, referred to as bePTFE because of a 'brushed' luminal treatment. This material offers a higher smooth surface area for cell attachment and deeper spaces to protect seeded cells from dislodgement due to blood flow (Figure 3). While standard ePTFE is seen to present a roughly 1:1 nodal:fibrillar surface area distribution (this depends on degree of longitudinal distention), this ratio for bePTFE is estimated to be in the range of 2:1 to 4:1. This change in solid surface area is a prominent feature of the bePTFE material, and it is believed to form as a result of a lifting up and smearing effect of the brush bristles on the node structures. Removal of luminal fibrillar material is another likely contributing factor. The 15-30 $\mu$ m deep grooves are clearly of appropriate

dimension to shield cells from the forces of blood flow. As shown by SEM (Figure 13D) cells are seen to be tucked between the raised nodes of the bePTFE yet and are more exposed when seen on either node or fibrillar regions on standard ePTFE (Figure 13A). These structural differences are believed to be behind the consistently observed higher cell uptake on the bePTFE material and the trend for seeded cells to be retained under pulsatile flow conditions (Figure 9).

Contact angle and ESCA data indicate that the physical manipulation of ePTFE into bePTFE using the controlled brushing process did not introduce any change in the material chemistry. Contact angle measurements were similar on each material and consistent with values reported in the literature for the hydrophobic ePTFE and PTFE material. ESCA data likewise demonstrated the surfaces to present concentrations of C and F consistent with PTFE. High resolution analysis on the C1s and F1s photoelectron peaks showed a gaussian C1s peak with binding energy of 292.5eV representative of CF<sub>2</sub> species. Only C and F were detected on all test areas of standard ePTFE. Similar results were obtained on bePTFE samples. A trace amount of oxygen at the detection limit and of unknown origin was observed on one of the test samples of bePTFE. This sample was identified to have been taken from an area of potentially more handling i.e., close to one end of the manufactured piece, and is considered to be a minor irregularity.

In contrast to the surface chemistry analysis, comparison of physical properties of ePTFE and bePTFE materials identified a number of differences. Comparison of moduli from

either circumferential or longitudinal stress-strain analyses showed an approximate 20% reduction associated with bePTFE. The estimate of material porosity from the Gurley measurement also showed a significant more rapid passage of air suggesting less resistance from a more porous material. The water entry pressure test, however, could not confirm any difference. Taken together, these results indicate the bePTFE material to have a reduced strength and increased porosity compared to ePTFE. The brushing process itself, and the eversion and re-eversion are the likely basis for this finding. In terms of physical appearance before and after implantation and general handling and suturability, no gross differences were apparent. Careful examination of bePTFE can, however, reveal faint longitudinal grooves believed to result from regular uneven bristles in the rotating Nylon wheel brush treatment.

To impart a rapid, simple, and even distribution of endothelial cells on the vascular graft surfaces we introduced the concept of axial centrifugal cell seeding using a modified-rotor centrifuge system. Technically the modified system had identical operation to the unmodified centrifuge, and the system (Figure 5) effectively imparted axial centrifugation to grafts containing cell suspensions. Notably, cells of numerous types safely experience a wide range of handling and g-forces conditions in cell separation, isolation, and concentration processes used today. For example, centrifugation of cell suspensions at 1000g for 15 minutes is common in the tissue culture suite, and, 1000-3000g 10-minute centrifugations are routinely used for blood separation in hematology laboratories. Interestingly, clinical blood separation itself saw a brief period of axial



centrifugation involving 2400g 1-minute centrifugation [25]. Examining target g-forces of 50, 250, and 500g, in 5-10 minute centrifugations, we observed endothelial cell uptake on graft materials to appear to plateau between 250-500g (Figure 9A). From this observation, a 250g 10 minute centrifugation was taken to be standard procedure. As mentioned, retaining the protective centrifuge lid was the limiting factor for the height of the rotor modification. This factor alone dictated the length of test graft specimens studied throughout this investigation. To demonstrate feasibility of this approach for use on grafts of more common clinical dimension, an OR-prototype axial centrifuge capable of centrifugation of grafts up to 6 mm ID and 60 cm length was designed and built (data not shown). This instrument was also based on the Eppendorf Model 5416 centrifuge. The final model, though longer and horizontally oriented, maintained the same operational features of the original instrument. For functionality in an operating room, the presentation of the vascular grafts was in a long sterile polycarbonate centrifuge tube with injection ports at each end for injecting hydration fluids and the cell suspension. The grafts also contained the same external sleeve for dehydration/handling protection.

The series of in vitro studies designed to identify factors influential to endothelial cell uptake/seeding and growth resulted in a number of significant findings. Under axial centrifugal g-force cell seeding the bePTFE material consistently showed high levels of cell uptake compared to the non-modified ePTFE (Figure 9B). This is believed to be due to the combination of the 2-4 fold greater smooth surface area on bePTFE for cells to establish focal adhesions, and the deep grooves that may act to protect the cells from

dislodgement due to a shielding effect. In addition, the level of g-force applied had a significant impact on the cell uptake on the graft surfaces. In the extreme case, when comparing simple slow rotation at the bench top i.e., “1 g”, to axial centrifugal seeding at 250g, very few cells are observed to be taken up by either material under the former condition (Figure 9B). However, generally 50-100 percent cell uptake can be observed in g-force seeding. The impact of hydration was also interesting in that a clear and unexpected interaction was observed: cell up take on standard ePTFE was significantly impacted by the state of graft hydration (uptake reduced on non-hydrated grafts) while this effect was not significant on bePTFE (Figure 9C). The cause behind this finding is unclear. With cell uptake being highest on either material in the bulk hydrated state, exposure of the non-hydrated bePTFE material to a cell suspension, with or without applied g-force, may have a higher potential to form a thin surface hydration layer similar to that seen in bulk hydration. Regarding incubation time i.e., the period of time allowed for g-force seeded cells to acclimate to the material before actual measurement of cell uptake, it is not surprising that adding an incubation period results in a trend for improved cell uptake. During this period it is thought that the cells are in a recovery period, loosely adherent, and in the early stages of making focal adhesions. Looking at the influence of flow, experiments to compare cell retention under pulsatile flow conditions showed that both the ePTFE and bePTFE appear to retain the cells received by g-force centrifugation following one hour of exposure to pulsatile flow (Figure 9D).

Five-day tissue culture studies on graft pre-seeding treatments intended to support the cell growth revealed that only material treatment with Matrigel or platelet poor plasma (PPP) was associated with a significant positive cell growth following seeding (Table 2). More significant perhaps was the observation that the order of applying PPP and cells was found to be important. Centrifugal cell seeding followed by coating with PPP, and the concomitant seeding in a suspension with PPP, showed inability of cells to thrive and significant cell loss. Only applying endothelial cells on top of a layer of PPP showed significant (and the highest) cell growth. Along with poor adhesion, this finding may shed some light on the mixed results of early cell seeding studies involving combination of endothelial cells with autologous blood used in graft pre-clotting procedures. This also likely reflects the degree of perturbation experienced by these cells which are designed and accustomed to living in the two dimensional environment - of basement membrane on one side and flowing blood on the other.

The use of both PPP and PRP generated from rapid OR and bedside sterile preparation systems have been receiving increasing attention in various applications in wound care management [26, 27]. Reports have documented that PRP, and on a lesser scale PPP, present a concentration of non-activated platelets and a rich blend of factors associated with tissue healing. These factors include transforming growth factor  $\beta$ , basic fibroblast growth factor, platelet-derived growth factor, epidermal growth factor, vascular endothelial growth factor, and connective tissue growth factor [28]. A number of these same factors also possess angiogenic and mitogenic activity that promote the population

of wound sites with various cells associated with general wound healing and angiogenesis [29]. The extent of the graft healing response to graft pretreatment with PPP as a growth medium has been an interesting finding. The original intention was to apply PPP, rather than platelet rich plasma, to lightly coat the material and avoid saturating the surfaces with cellular material, as this would form a barrier to the deposit of endothelial cells onto the surfaces. This we thought would provide seeded cells with sufficient adhesive proteins for cell uptake and growth, yet also allow opportunity for interaction with the surfaces and allow careful comparison of responses to the different material surface topographies. We believe that because the hydration process saturated the graft interstices with EBM-2 media containing calcium, the concentration gradient of  $\text{Ca}^{2+}$  between the media and the citrated (decalcified) PPP drove  $\text{Ca}^{2+}$  transport into PPP at the material interface. The  $\text{Ca}^{2+}$ , a critical cofactor in the coagulation process, reached a sufficient concentration to activate local coagulation activity and result in a local formation of an autologous fibrin-platelet poor layer (aFPPL) at the surface. The aFPPL often masked the surfaces, and appeared to form a 2-30 $\mu$  thick layer of varying fibrin density (Figure 19). This variation is related to differences in the subject PPP, which is a function of hematocrit, platelet count, and subject coagulation potential [30]. The 4-5 fold increase in in vitro growth of cells that are centrifugal-seeded on top of an aFPPL suggests the material is indeed rich in factors promoting endothelial cell growth. The composition of an aFPPL is presumed to be markedly richer in these factors compared to the commercially-available fibrin kits used to pre-treat grafts in the current two stage method (material derived from platelet-free processed pooled human plasma). The

composition can also be presumed to be very different from cases where pre-clotting is performed on vascular grafts, which would necessarily include high levels of active thrombin and more cellular (primarily RBC) mass. The aFPPL itself, or a combined effect with exuberant healing in the canine model, is believed to have played a significant role in the in vivo observation where PPP treatment alone showed significant endothelialization in the absence of endothelial cell seeding.

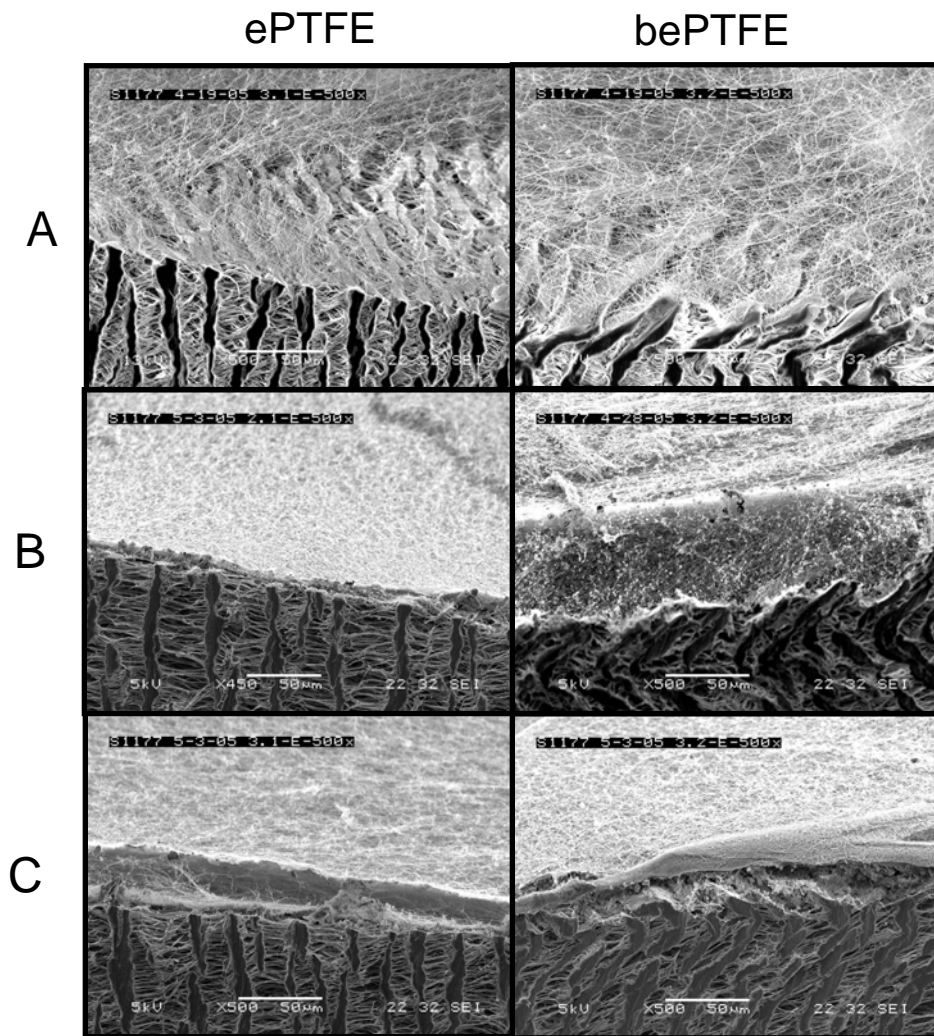


**Figure 19.** Representative SEM micrographs showing an on-edge cut revealing the variation in morphology and thickness of the autologous fibrin-platelet-poor layer (aFPPL). A,B, and C represent approximately thin, intermediate, and thick aFPPLs.

The healing of synthetic grafts in humans has been described as being very limited, with anastomotic outgrowth of native endothelium typically restricted to the first centimeter past the anastomoses [31-33]. In contrast, it has been suggested by many that complete endothelialization of synthetic grafts occurs naturally in animal models, particularly when using short lengths of test grafts [31-34]. This apparent dichotomy can confound investigations using animal models to study the potential effectiveness of endothelial cell seeding in humans. A critical factor in the concluding in vivo pilot study was therefore to demonstrate a *lack* of endothelialization in the non-treated control grafts. Previous unpublished experience using standard ePTFE as a routine control graft suggested that endothelialization of ePTFE grafts in the canine model may not be as vigorous as often suggested. This experience revealed that endothelial outgrowth can occur unevenly from each anastomosis, and, over long periods of time (up to one year) it can also proceed unevenly down a graft lumen. The latter can even leave some areas bare of endothelium and some areas showing a well developed neointima. This experience suggested that evaluation of 4-cm long 4 mm ID grafts after a 6-week implant duration would show an absence of endothelial cells in the midgraft region. In this study, histology observations (Figure 15) and SEM observations (Figure 17) confirmed that midgraft regions of each non-treated graft material reveal either a bare or predominantly fibrin-platelet surface devoid of endothelial cells. The coverage of this pseudointimal surface is further demonstrated in Figure 20 which depicts extent of endothelial outgrowth determined by

SEM scoring for endothelium on all control grafts. Here, endothelium from anastomotic outgrowth generally did not extend past 14 mm (around region 4) from the proximal anastomoses and 10 mm past the distal anastomosis (around region 8). From these observations it was presumed that the presence and extent of endothelial cells in the midgraft region would be a result of cell seeding. Positive or negative interactions between cell seeding and PPP pretreatment and/or the type of underlying graft material were estimated to be feasible.

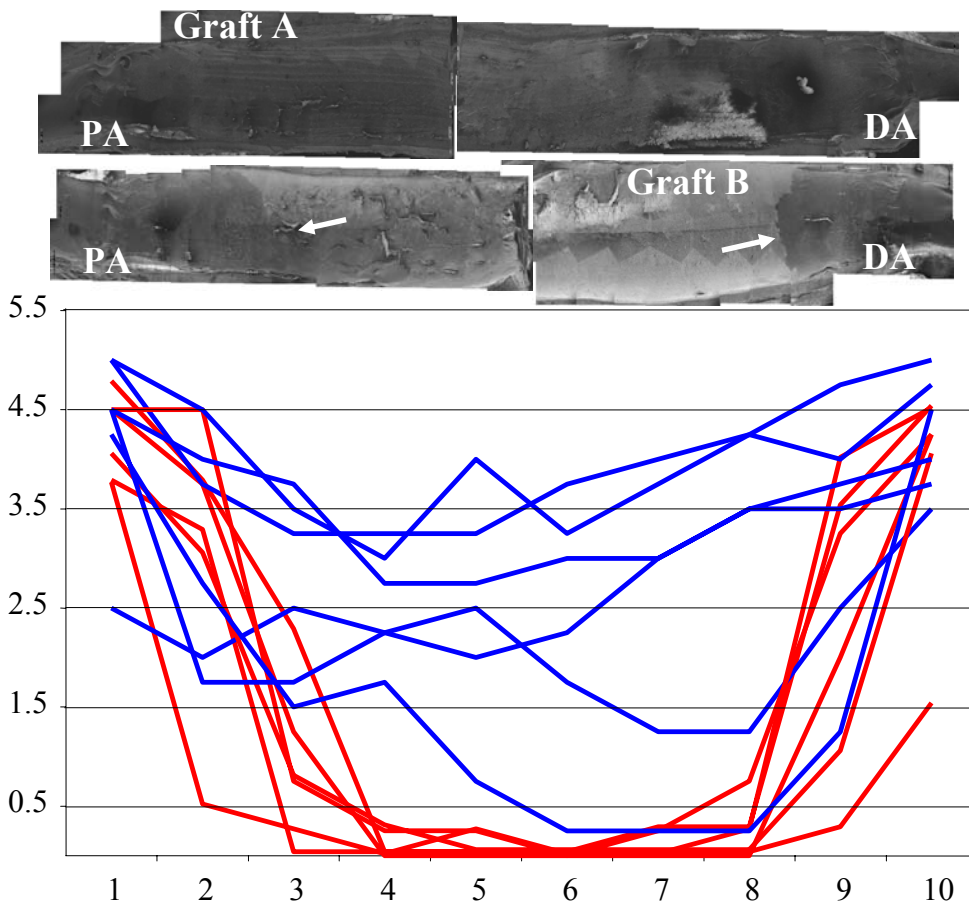


**Figure 20.** Representative SEM montages of a bePTFE control explant (A) and ePTFE control explant (B). The arrow indicates the obvious leading edge of anastomotic outgrowth on the ePTFE graft. The average SEM scores along these explants and the other patent control grafts are shown in red. The blue lines show the average SEM scores for along each explant receiving both PPP treatment and cell seeding.

Statistical analysis of patent versus non-patent grafts failed to identify any of the study factors as having a statistically significant impact on patency. This finding was anticipated as ePTFE grafts in this model typically achieve patencies on the order of 75-100%. With high patencies necessitating large numbers of animals to determine statistical significance, researchers often look to features of the healing response to help distinguish favorable and unfavorable attributes. Here, of the 32 vascular grafts implanted in the study, the study fell in the expected patency range with 10/16 patent ePTFE grafts and 14/16 patent bePTFE grafts (Table 3). As noted, these results include four animals presenting unilateral graft occlusion and two animals presenting bilateral occlusions. The latter grafts were suspected to involve graft infection. With all graft test conditions implanted in duplicate, the failures fortunately did not involve loss of any duplicate conditions. In spite of the small sample size and expected low power in a binomial patency analysis, it may be noteworthy that the exact logistic test did determine that two of the study factors came close to being statistically significant: material ( $P < 0.07$ ) and cell seeding ( $P < 0.08$ ). While the numbers suggest a trend, in hindsight the replacement of the infected animals would have aided to elucidate whether or not the modified ePTFE material offers a significant impact on patency. The significance of the cell seeding factor comes obviously not from the equal patencies in the seeded versus non seeded groups (12/16). Rather, it comes from the potential interaction between these factors in that all (8/8) bePTFE grafts receiving cell seeding were patent compared to only four (4/8) seeded ePTFE grafts. With the endothelial cell harvesting procedure



showing significant variation in cell stripping efficiency (Figure 11) and ultimate widely varying seeding densities, improvements in this step of the process could give rise to higher seeding densities and/or reduced trauma to cells. Such improvements would be expected to impact the patency statistics. Poor and varying cell harvesting alone, and/or in combination with loose initial adherence following static seeding likely contributed to the mixed results observed throughout initial trials in endothelial cell seeding. Regarding the impact of the directionality of the bePTFE grafts on patency, no gross differences were obvious on patent grafts and that within the two graft failures, one graft of each orientation was involved.

General gross inspection of graft explants showed graft lumens range in appearance from a smooth glistening white to completely covered in organizing red thrombus (representative images of patent grafts seen in Figure 14). This enticed us to conduct a blinded scoring of the degree of red coloration, or potential red thrombus, observed in patent grafts. ANOVA analysis on the scores yielded each factor i.e., material, cell seeding, and PPP treatment to each have a significant ( $P \ll 0.05$ ) impact on the observation. Generally the bePTFE grafts, cell seeded grafts, and PPP treated grafts revealed lowest scores on this observation. A caveat in this simple analysis is that not all red deposits were carefully scrutinized for consistency with active thrombosis. Some on the red coloration, for example, may come from red blood cells worked into the luminal interstices of the ePTFE material or bePTFE groves, and may therefore not be a component of an active thrombotic process taking place.

ANOVA analysis on the histological scores revealed that seeding with endothelial cells was the only factor demonstrating a significant impact on one or more histological response categories. Here, cell seeding was seen to have a significant impact ( $P < 0.05$ ) on extent of neointimal formation, overall material cellularity, and macrophage infiltration. In each case a higher level of the response was associated with implants that received cell seeding. The study was not carried out long enough to determine the implication of a higher macrophage response, but this would be an obvious point of scrutiny in follow-up studies. The question of whether macrophages are friends or foes in prosthetic graft healing seems to be indicating they can be both i.e., friends at the beginning and foes at the end [34]. For the categories of thrombosis, acute and chronic inflammation, and anastomotic hyperplasia, neither graft material nor graft pretreatment with PPP appeared to have a significant influence. However, it may be noteworthy that thrombosis and cellularity scores showed marginal dependence on the type of graft material present ( $P < 0.08$  and  $P < 0.09$ , respectively). Here, bePTFE tended to show less thrombus, which was consistent with the discoloration scores and patency data, and more cellularity in the graft interstices. Normally, cells associated with graft healing e.g., fibroblasts, monocytes, macrophages, have a difficult time penetrating the small and very dense internodal and interfibrillar spaces in ePTFE. As shown in the material characterization studies, bePTFE appears to be more porous by air permeability testing. Thus, a higher degree of cellularity would be anticipated. Histological images also generally reveal that regardless of type of graft, grafts without PPP treatment or cell

seeding reveal a barren non-cellular midgraft. Grafts that received either PPP treatment alone or in combination with cell seeding reveal a thin cellular lining consistent with endothelium. The thickness of the latter neointimal linings was highly variable, but showed a trend for being slightly thicker on bePTFE (Figure 15). In addition, in the cases where bePTFE was oriented towards or against the flow, no differences in appearances were apparent.

Finally, as noted throughout this work, factorial experimental design (FED) approach [35, 36]. was used to (1) rapidly ascertain which factors influenced the outcome of endothelial cell seeding studies, and (2) determine what levels of the factors had the greatest impact. Given the host of variables potentially affecting the efficiency and fate of endothelial cells seeded onto vascular graft materials, the use of a one-variable-at-a-time (OVAT, or OFAT = one-factor-at-a-time) approach to study this complex topic was seen to be inefficient, unwieldy and cost and time prohibitive. Given that FED approach is receiving increasing attention as a means to screen multiple factors for importance while limiting the use of experimental animals [37, 38] we also applied FED in the concluding in vivo study. As seen in the study, not one but four potentially significant variables were examined simultaneously against a series of commonly used explant analyses. It remains to be seen if the modified bePTFE material can be a significant factor for better graft endothelialization from seeding, yet measurements such as high cell uptake under centrifugal cell seeding, trend in patency, and luminal appearance suggest a favorable influence. Moreover, in examining autologous PPP treatment alongside

endothelial cell seeding, we were able to see that such an extra step in an OR procedure may be insignificant, as midgraft endothelium seems similar without this treatment. Alternatively, if humans had potential to heal like canines, and there are case examples endothelialized grafts in humans [39-41], the application of a rapidly-generated growth matrix of autologous PPP or PRP may be highly significant since it appeared in these studies that the resulting aFPPL layer had an acceleration effect on endothelialization in the absence of seeding with endothelial cells. Clearly, more work needs to be directed at better this observation, and at deciphering the frequent claims of dramatically different healing responses between animals and humans.

In conclusion, efforts here to re-examine a one stage cell seeding process found that axial centrifugation was a rapid and efficient means to apply endothelial cells evenly onto graft surfaces. The method showed efficient cell uptake and retention on the ePTFE graft materials compared to static or slow rotation methods. And, cells seeded in this fashion appeared to better hold onto the surfaces under pulsatile conditions. In vitro studies showed the special modified bePTFE material to present some unique physical features and favorable responses, such as consistently higher cell uptake. However, in vivo findings with bePTFE vascular grafts were favorable, yet inconclusive. A schematic of the new process is shown in Figure 21. The scaling up of this approach for use in an operating room was suggested. The method envisioned would involve an OR tabletop axial centrifuge capable of handling all common graft sizes. Presentation of a graft would be in the form of a sterile disposable centrifuge tube. Graft preparation would then

be through injection ports at either end, simple injection of pre-prepared syringes of wetting solutions, possible injection of autologous PPP to create an aFPPL, and an appropriate endothelial cell suspension. Significantly, this work only examined autologous venous endothelial cells removed from venous tissue using a clinically tested method. Constraints on the methodology and available of alternative technology did not allow for treatment of seeding density and alternative cell sources as variables. With commonly implanted synthetic grafts (particular peripheral grafts) greatly exceeding the size of graft examined in these studies, complete cell coverage on the order of  $300,000/\text{cm}^2$  (Figure 4) may require a richer alternative source of endothelial cells for this seeding concept. Further progress towards a successful one-stage OR procedure may then hinge upon coupling concepts such as those proposed here, with alternative cell sources, such as adipose-derived endothelial cells [42, 43] and circulating endothelial progenitor cells [44-46].

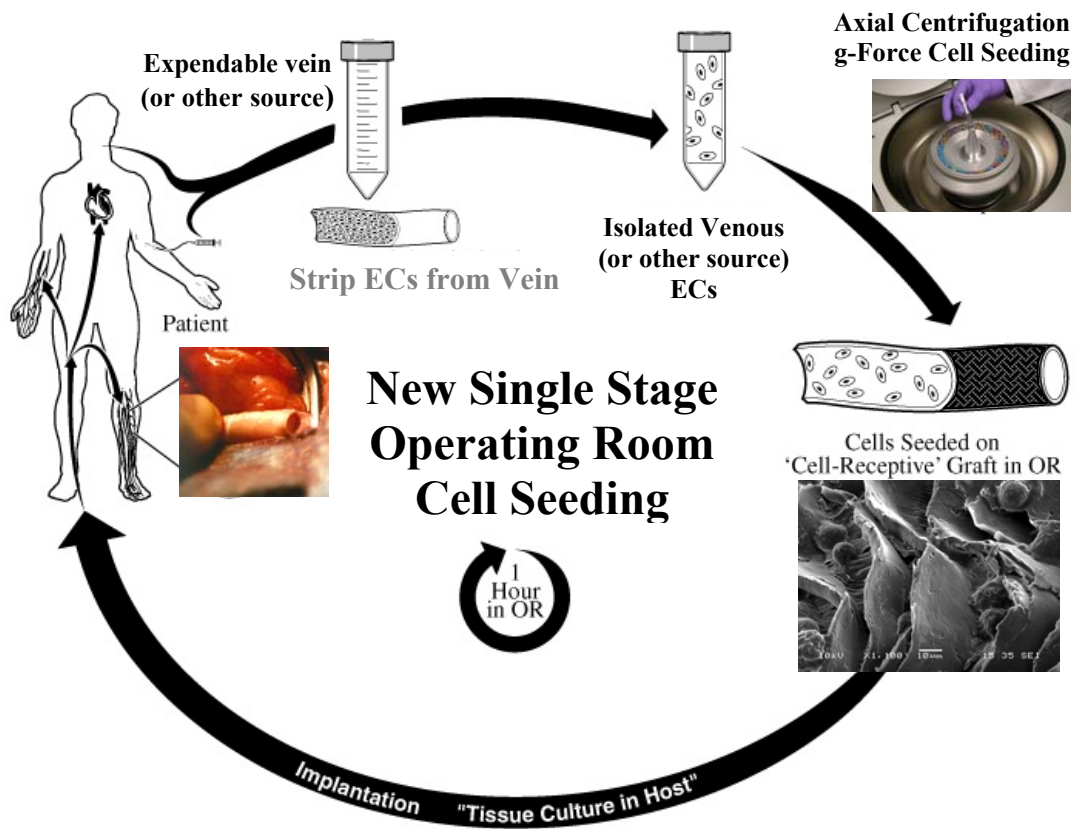


**Figure 21.** Schematic representation of a possible practicable new single-stage approach to seeding synthetic grafts in the operating room with autologous cells. Here, an adequate number of endothelial cells are obtained from a source using minimally invasive procedure. The cells are the applied using axial centrifugation g-force seeding onto a graft that is receptive to these cells. The graft is then immediately implanted and a confluent endothelium arises within 4-6 weeks post implantation.

## BIBLIOGRAPHY

- [1] Mansfield PB, Wechezak AR, Sauvage LR. Preventing thrombus on artificial vascular surfaces: true endothelial cell linings. *Trans Am Soc Artif Intern Organs* 1975;21:264-72.
- [2] Herring M, Gardner A, Glover J. A single-staged technique for seeding vascular grafts with autogenous endothelium. *Surgery* 1978;84(4):498-504.
- [3] Bordenave L, Fernandez P, Remy-Zolghadri M, Villars S, Daculsi R, Midy D. In vitro endothelialized ePTFE prostheses: clinical update 20 years after the first realization. *Clin Hemorheol Microcirc* 2005;33(3):227-34.
- [4] Vara DS, Salacinski HJ, Kannan RY, Bordenave L, Hamilton G, Seifalian AM. Cardiovascular tissue engineering: state of the art. *Pathol Biol (Paris)* 2005;53(10):599-612.
- [5] Seifalian AM, Tiwari A, Hamilton G, Salacinski HJ. Improving the clinical patency of prosthetic vascular and coronary bypass grafts: the role of seeding and tissue engineering. *Artif Organs* 2002;26(4):307-20.
- [6] Meinhart JG, Deutsch M, Fischlein T, Howanietz N, Froschl A, Zilla P. Clinical autologous in vitro endothelialization of 153 infrainguinal ePTFE grafts. *Ann Thorac Surg* 2001;71(5 Suppl):S327-31.
- [7] Laube HR, Duwe J, Rutsch W, Konertz W. Clinical experience with autologous endothelial cell-seeded polytetrafluoroethylene coronary artery bypass grafts. *J Thorac Cardiovasc Surg* 2000;120(1):134-41.
- [8] Sandhu HS. Bone morphogenetic proteins and spinal surgery. *Spine (Phila Pa 1976)* 2003;28(15 Suppl):S64-73.
- [9] Zilla P, Fasol R, Dudeck U, Siedler S, Preiss P, Fischlein T, Muller-Glauser W, Baitella G, Sanan D, Odell J and others. In situ cannulation, microgrid follow-up and low-density plating provide first passage endothelial cell masscultures for in vitro lining. *J Vasc Surg* 1990;12(2):180-9.
- [10] Zilla P, Fasol R, Preiss P, Kadletz M, Deutsch M, Schima H, Tsangaris S, Groscurth P. Use of fibrin glue as a substrate for in vitro endothelialization of PTFE vascular grafts. *Surgery* 1989;105(4):515-22.
- [11] Herring M, Baughman S, Glover J. Endothelium develops on seeded human arterial prosthesis: a brief clinical note. *J Vasc Surg* 1985;2(5):727-30.
- [12] Fischlein T, Zilla P, Meinhart J, Puschmann R, Vesely M, Eberl T, Balon R, Deutsch M. In vitro endothelialization of a mesosystemic shunt: a clinical case report. *J Vasc Surg* 1994;19(3):549-54.
- [13] Deutsch M, Meinhart J, Vesely M, Fischlein T, Groscurth P, von Oppell U, Zilla P. In vitro endothelialization of expanded polytetrafluoroethylene grafts: a clinical case report after 41 months of implantation. *J Vasc Surg* 1997;25(4):757-63.

- [14] Kips Bay Medical; Seeding Implantable Medical Devices with Cells. United States Patent Application US2007/0059335, 2007.
- [15] Rosenman JE, Kempczinski RF, Pearce WH, Silberstein EB. Kinetics of endothelial cell seeding. *J Vasc Surg* 1985;2(6):778-84.
- [16] Kesler KA, Herring MB, Arnold MP, Glover JL, Park HM, Helmus MN, Bendick PJ. Enhanced strength of endothelial attachment on polyester elastomer and polytetrafluoroethylene graft surfaces with fibronectin substrate. *J Vasc Surg* 1986;3(1):58-64.
- [17] Williams SK, Rose DG, Jarrell BE. Microvascular endothelial cell seeding of ePTFE vascular grafts: improved patency and stability of the cellular lining. *J Biomed Mater Res* 1994;28(2):203-12.
- [18] Fields C, Cassano A, Makhoul RG, Allen C, Sims R, Bulgrin J, Meyer A, Bowlin GL, Rittgers SE. Evaluation of electrostatically endothelial cell seeded expanded polytetrafluoroethylene grafts in a canine femoral artery model. *J Biomater Appl* 2002;17(2):135-52.
- [19] Soletti L, Nieponice A, Guan J, Stankus JJ, Wagner WR, Vorp DA. A seeding device for tissue engineered tubular structures. *Biomaterials* 2006;27(28):4863-70.
- [20] Chen HC, Hu YC. Bioreactors for tissue engineering. *Biotechnol Lett* 2006;28(18):1415-23.
- [21] Salacinski HJ, Tiwari A, Hamilton G, Seifalian AM. Cellular engineering of vascular bypass grafts: role of chemical coatings for enhancing endothelial cell attachment. *Med Biol Eng Comput* 2001;39(6):609-18.
- [22] ANSI/AAMI/ISO 7198: 1998. Cardiovascular implants—Tubular vascular prostheses. 3rd ed. Arlington, VA: Association for the Advancement of Medical Instrumentation; 2001/(R) 2004.
- [23] Munch K, Wolf MF, Gruffaz P, Ottenwaelter C, Bergan M, Schroeder P, Fogt EJ. Use of simple and complex in vitro models for multiparameter characterization of human blood-material/device interactions. *J Biomater Sci Polym Ed* 2000;11(11):1147-63.
- [24] Bissel MJ, Aggeler J. Dynamic Reciprocity: How do Extracellular matrix and hormones direct gene expression? In: Cabot MC, McKeegan WL, editors; 1987 September 8-11, 1986; Lake Placid, New York. Alan Liss. p 321
- [25] Estey CA, Felder RA. Clinical trials of a novel centrifugation method: axial separation. *Clin Chem* 1996;42(3):402-9.
- [26] Khalafi RS, Bradford DW, Wilson MG. Topical application of autologous blood products during surgical closure following a coronary artery bypass graft. *Eur J Cardiothorac Surg* 2008;34(2):360-4.



- [27] Saratzis N, Saratzis A, Melas N, Kiskinis D. Non-activated autologous platelet-rich plasma for the prevention of inguinal wound-related complications after endovascular repair of abdominal aortic aneurysms. *J Extra Corpor Technol* 2008;40(1):52-6.
- [28] Everts PA, Knape JT, Weibrich G, Schonberger JP, Hoffmann J, Overdeest EP, Box HA, van Zundert A. Platelet-rich plasma and platelet gel: a review. *J Extra Corpor Technol* 2006;38(2):174-87.
- [29] Anitua E, Andia I, Ardanza B, Nurden P, Nurden AT. Autologous platelets as a source of proteins for healing and tissue regeneration. *Thromb Haemost* 2004;91(1):4-15.
- [30] Kaplan S, Marcoe KF, Sauvage LR, Zammit M, Wu HD, Mathisen SR, Walker MW. The effect of predetermined thrombotic potential of the recipient on small-caliber graft performance. *J Vasc Surg* 1986;3(2):311-21.
- [31] Wesolowski SA, Fries CC, Hennigar G, Fox LM, Sawyer PN, Sauvage LR. Factors Contributing to Long-Term Failures in Human Vascular Prosthetic Grafts. *J Cardiovasc Surg (Torino)* 1964;5:544-67.
- [32] Berger K, Sauvage LR, Rao AM, Wood SJ. Healing of arterial prostheses in man: its incompleteness. *Ann Surg* 1972;175(1):118-27.
- [33] Herring M. Endothelial Seeding of Blood Flow Surfaces. In: Wright CB, editor. *Vascular grafting: Clinical Applications and Techniques*. Boston: J. Wright, PSG Inc.; 1983. p 275.
- [34] Zilla P, Bezuidenhout D, Human P. Prosthetic vascular grafts: wrong models, wrong questions and no healing. *Biomaterials* 2007;28(34):5009-27.
- [35] Montgomery DC. *Design and analysis of experiments*. Hoboken, NJ: Wiley; 2008. xvii, 656 p.
- [36] Box GEP, Hunter JS, Hunter WG. *Statistics for experimenters : design, innovation, and discovery*. Hoboken, N.J.: Wiley-Interscience; 2005. xvii, 633 p.
- [37] Shaw R, Festing MFW, Peers I, Furlong L. Use for Factorial Designs to Optimize Animal Experiments and Reduce Animal Use. *ILAR* 2002;43(4):223-232.
- [38] Festing MFW, Overend P, Gaines-Das R, Cotina-Borja M, Berdoy M. *The Design of Animal Experiments: Reducing the Use of Animals in Research Through Better Experimental Design*. London: Royal Society of Medicine Press (RSM), for Laboratory Animals, Ltd.; 2004. 116 p.
- [39] Wu MH, Shi Q, Wechezak AR, Clowes AW, Gordon IL, Sauvage LR. Definitive proof of endothelialization of a Dacron arterial prosthesis in a human being. *J Vasc Surg* 1995;21(5):862-7.
- [40] Sauvage LR, Berger K, Beilin LB, Smith JC, Wood SJ, Mansfield PB. Presence of endothelium in an axillary-femoral graft of knitted Dacron with an external velour surface. *Ann Surg* 1975;182(6):749-53.

- [41] Shi Q, Wu MH, Onuki Y, Ghali R, Hunter GC, Johansen KH, Sauvage LR. Endothelium on the flow surface of human aortic Dacron vascular grafts. *J Vasc Surg* 1997;25(4):736-42.
- [42] Williams SK, Jarrell BE, Rose DG, Pontell J, Kapelan BA, Park PK, Carter TL. Human microvessel endothelial cell isolation and vascular graft sodding in the operating room. *Ann Vasc Surg* 1989;3(2):146-52.
- [43] Williams SK. Human Clinical Trials of Microvascular Endothelial Cell Sodding. In: Zilla P, Greisler HP, editors. *Tissue Engineering of Vascular Prosthetic Grafts*. Austin, TX: Landes Bioscience; 1999. p 143-147.
- [44] He H, Shiota T, Yasui H, Matsuda T. Canine endothelial progenitor cell-lined hybrid vascular graft with nonthrombogenic potential. *J Thorac Cardiovasc Surg* 2003;126(2):455-64.
- [45] Khoo CP, Pozzilli P, Alison MR. Endothelial progenitor cells and their potential therapeutic applications. *Regen Med* 2008;3(6):863-76.
- [46] Ben-Shoshan J, George J. Endothelial progenitor cells as therapeutic vectors in cardiovascular disorders: from experimental models to human trials. *Pharmacol Ther* 2007;115(1):25-36.